CFD Activities at NASA Langley

Mujeeb.R. Malik@NASA.GOV
Research Directorate
NASA Langley Research Center
Hampton, VA

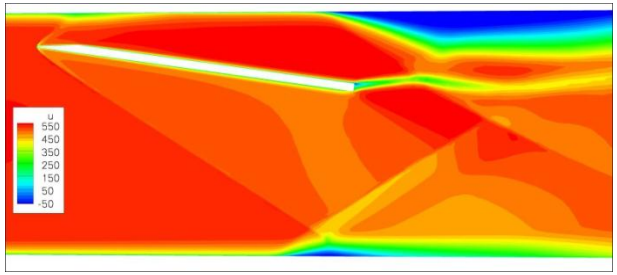

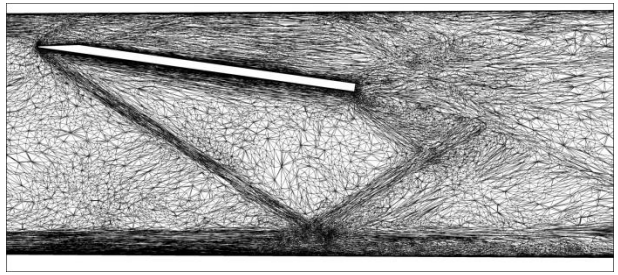

DLR, Braunschweig
June 7, 2010

Outline

- **Introduction to NASA Langley**
- **CFD Codes**
  - *For Subsonic to Hypersonic Applications*
- **CFD Methods Development**
  - *FUN3D*
  - *Grid Adaptation*
  - *Cell centered vs. node centered schemes*
  - *Multidimensional flux reconstruction*
  - *Design optimization using unsteady adjoint*
  - *High-order methods*
- **Unsteady Simulations**
  - *Airframe noise source computations*
- **BL Transition Research**
  - *Roughness effect*
- **Concluding Remarks**

Fundamental Aeronautics and Integrated Systems Research Projects

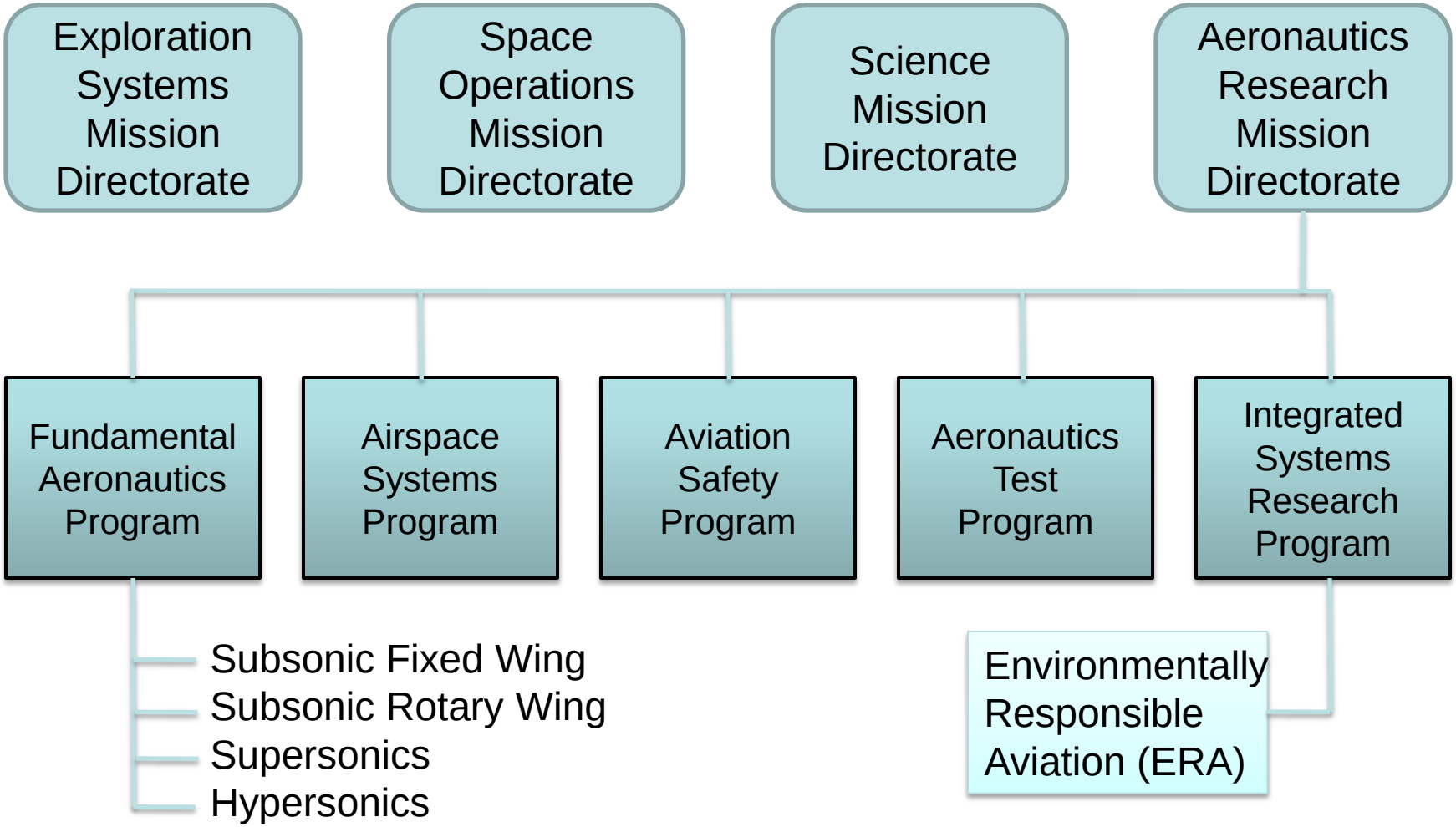

NASA Langley at a Glance (2009)

Infrastructure/Facilities

- 788 acres, 241 Buildings
- $2.7B replacement value

Founded in 1917
1st civil aeronautical research laboratory

~$746M Budget
~$731M NASA Langley budget
~$15M External business

~3,500 Workforce
~1,900 Civil Servants
~1,600 Contractors (on/near-site)
~250 students

Aeronautics $165M	Exploration $133M	Science $76M	Space Operations $3M	Cross Agency Programs $33M	Other Mission Support $102M	Center Management & Operations $219M

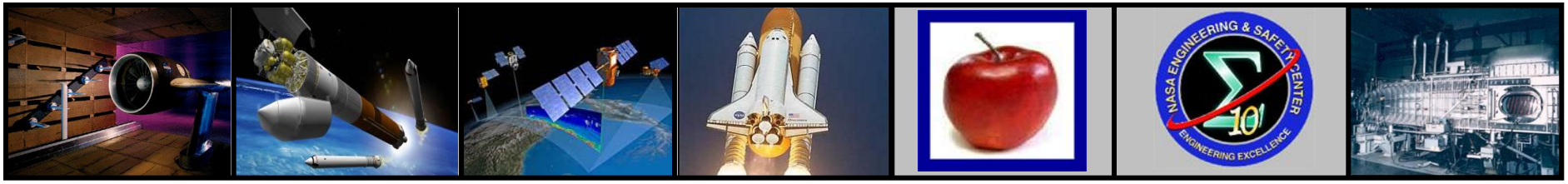

NASA Langley Research Center Organization

OUR MISSION: LaRC Pioneers the Future in Space Exploration, Scientific Discovery, and Aeronautics Through Research and Development of Technology, Scientific Instruments, and Exploration Systems.

We Deliver on Today's Commitments and Prepare for Tomorrow's Opportunities

Agency Functions

NASA Engineering & Safety Center
Ralph R Roe Jr

Independent Program Office
Mark P Saunders

Director's Office

Director
Lesa B Roe

Deputy Director
Stephen G Jurczyk

Assoc. Director
Cynthia C Lee

Agency Programs

Science Support Office
Raleigh B Perry Jr

Exploration Technology Dev. Program Office
Frank Peri Jr

Mission

Aeronautics Research
Vicki K Crisp

Science
Lelia B Vann

Exploration and Space Operations
David E Bowles

Flight Projects
Luat T Nguyen

Systems Analysis and Concepts
Ajay Kumar

Ground Facilities and Testing
Damodar R Ambur

Advanced Planning and Partnership
Richard R Antcliff

Research Services
Howard J Lewis Jr

Systems Engineering
Stephen P Sandford

Research & Technology
Charles E Harris

Center Operations
George B Finelli

Mission Support

Safety & Mission

Systems

Procurement

Chief Counsel

Equal Opportunity
Janet E Sellars

Human Capital Management
Leah M Meisel

Strategic Communications & Education
Mark J Shuart

Chief Financial Officer
Kenneth J Winter

Chief Information Officer
Cathy H Mangum

Research Directorate

Business Support Team

D. T. Baxter , M. L. Sample, L. R. Williams
Business Managers

Lori W. Brown and Bonnie J. Lumanog
Administrative Officer

Jennifer Frost
Secretary

L. David Wall
Center Support Contracts Manager

Jamie W. Godsey
Information Technology Manager

Senior Leadership Team

Charles E. Harris, Director
Steven G. Reznick, Deputy Dir for Workforce Development
Edward A. Healy, Jr., Deputy Dir for Program Implementation
Brenton W. Weathered, Chief Engineer for Airborne Systems
Larry Leavitt, Chief Engineer for Aerosciences
W. Keith Belvin, Chief Engineer for Structures and Materials
Edward R. Generazio, Agency NDE Specialist
Mujeeb R. Malik, Senior Technical Advisor for Aerodynamics

Safety Professionals

Peter M. Kjeldsen,
Internal Quality Assessment Specialist
Charles B. Zeitman,
Safety and Occup Health Manager

Configuration Aerodynamics Branch
Zachary T. Applin, Head
Richard A. Wahls, Assist. Head
vacant, Assist. Head

Computational Aerosciences Branch
Joseph H. Morrison, Head
vacant, Assist Head

Flow Physics and Controls Branch
Anthony E. Washburn, Head
Catherine B. McGinley, Assist. Head

Advanced Sensing & Optical Measurement Branch
Kenneth D. Wright, Head
William M. (Tony) Humphreys, Assist. Head (Detailed)

Aerothermodynamics Branch
N. Ronald Merski, Head
Michael Difulvio, Assist. Head

Hypersonic Airbreathing Propulsion Branch
Kenneth E. Rock, Head
Shelly M. Ferlemann, Assist. Head

Advanced Materials and Processing Branch
Vacant, Head
Emilie J. Siochi , Acting Head
Erik S. Weiser, Assist. Head

Aeroelasticity Branch
Stanley R. Cole, Head
Boyd Perry III, Assist. Head

Durability, Damage Tolerance and Reliability Branch
Jonathan B. Ransom, Head
Edward H. Glaessgen, Assist. Head

Structural Mechanics and Concepts Branch
David N. Brewer, Head

Nondestructive Evaluation Sciences Branch
William P. Winfree, Head
D. Michele Heath, Assist. Head

Aeroacoustics Branch
Charlotte E. Whitfield, Head
Michael A. Marcolini, Assist. Head

Dynamic Systems and Control Branch
Marty Waszak, acting
Carey S. Buttrill, Head, Detail

Flight Dynamics Branch
Charles M. Fremaux, Head

Crew Systems and Aviation Operations Branch
Lisa O. Rippy, Head
James R. Comstock, Jr. , TL Crew Sys
Elliot T. Lewis, TL Aviation Operations

Electromagnetics and Sensors Branch
Erik Vedeler, Head

Safety-Critical Avionics Systems Branch
Raymond S. Calloway, Head
Eric G. Cooper, Acting Assist. Head

Structural Acoustics Branch
Kevin P. Shepherd, Head
Richard J. Silcox, Assist. Head

Structural Dynamics Branch
Vacant, Head

Materials Experiments Branch
Kelly S. Tarkenton, Head

Structures Experiments Branch
R. Scott Young, Head

NASA Langley's Aerodynamic/Propulsion/Aerothermo Computational Tool Set

High fidelity, credible aerodynamic/propulsion performance and aeroheating levels/loads required everywhere along flight trajectory

Subsonic *Supersonic* *Hypersonic* *Rarefied*

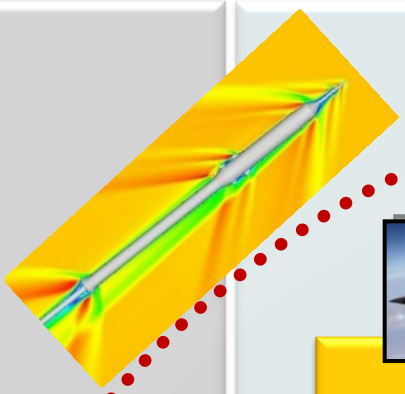

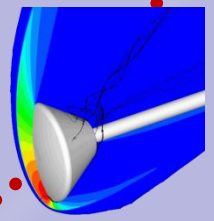

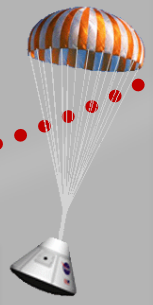

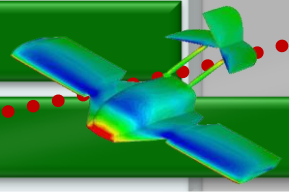

DAC - DSMC

HARA

LAURA

VULCAN

CFL3D

OVERFLOW

TetrUSS/USM3D

FUN3D

Aero

Heating

Aero & heating

Propulsion

Essential inputs to: Aerodynamics, structures, materials (thermal protection), GN&C, propulsion, operations, system integration

FUN3D Core Capabilities

http://fun3d.larc.nasa.gov

- Solves 2D/3D steady and unsteady Euler and RANS equations on node-based mixed element grids for compressible and incompressible flows; cell-centered schemes being investigated
- Supports numerous internal/external efforts across the speed range
- General dynamic mesh capability: any combination of rigid/overset/morphing grids, including 6-DOF effects
- Aeroelastic modeling w/ mode shapes, full FEM, CC, etc
- Constrained/multipoint adjoint-based design and mesh adaptation
- Modern software practices including 24/7 testing
- Linear scaling through thousands of cores

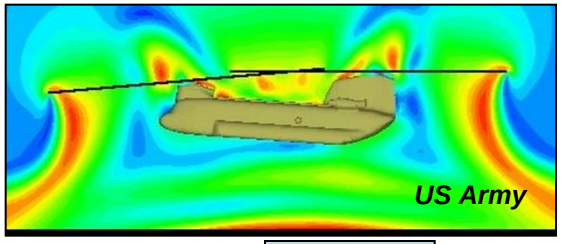

Rotorcraft

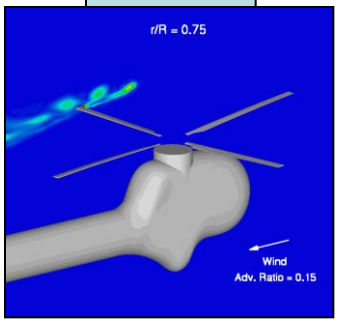

BMI Corporation

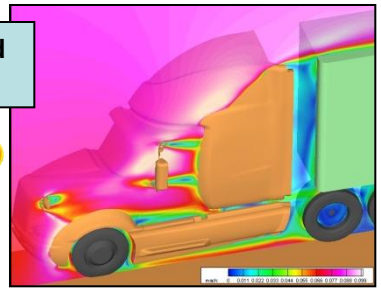

Low-Speed Flows

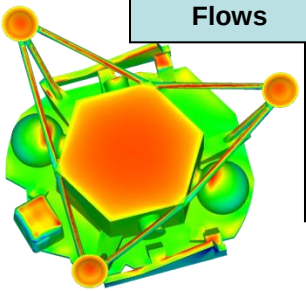

Morphing Vehicles

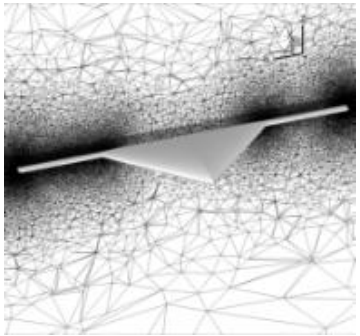

Ares

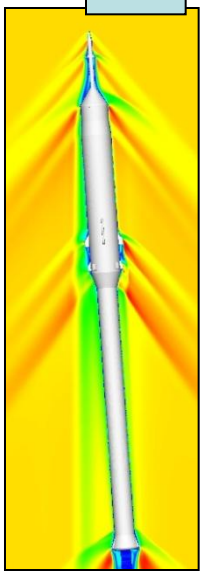

Reacting Flows

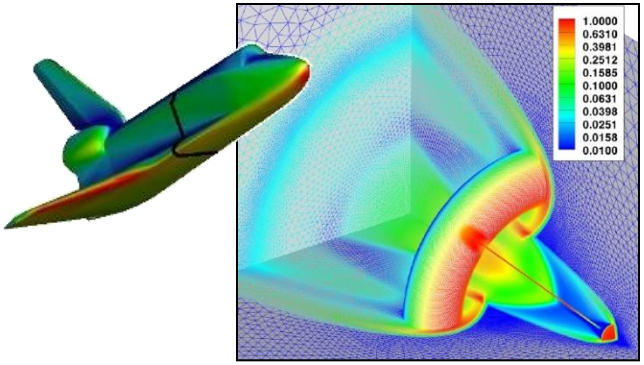

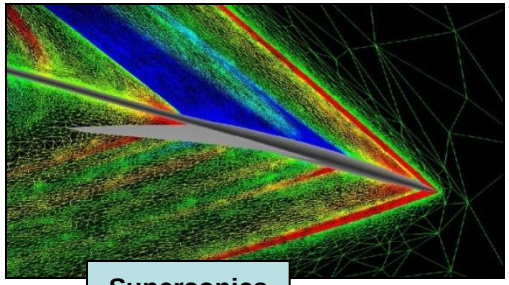

Supersonics

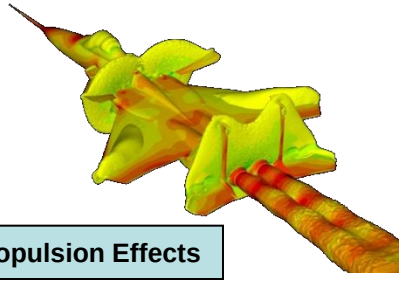

Propulsion Effects

FUN3D Computational Performance

- Effort initiated in 2006 to study and improve computational performance of solver
- Many low-level aspects examined
  - Cache reuse
  - MPI communication
  - Alternative ordering techniques for grid/linear algebra operations
  - Inlining
  - Basic blocks
- Experimented with hierarchical partitioning strategies; will revisit at higher core densities
- 6.5x speedup demonstrated (hardware, compiler and options held fixed)
- Linear scaling demonstrated to 8,192 cores on pleiades (queue becomes limiting factor)
- Working with Oak Ridge staff to continue improving massively parallel performance
  - Experimenting on ORNL Jaguar system (250,000 cores; #1 on Top500)

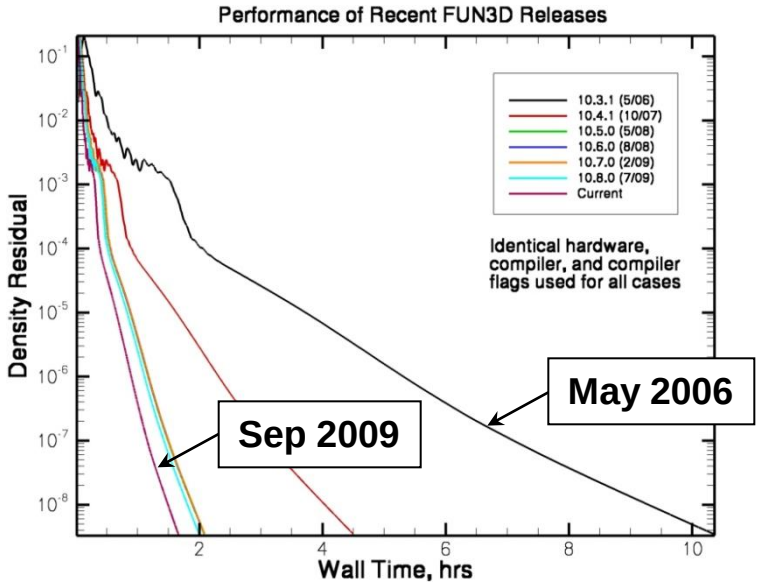

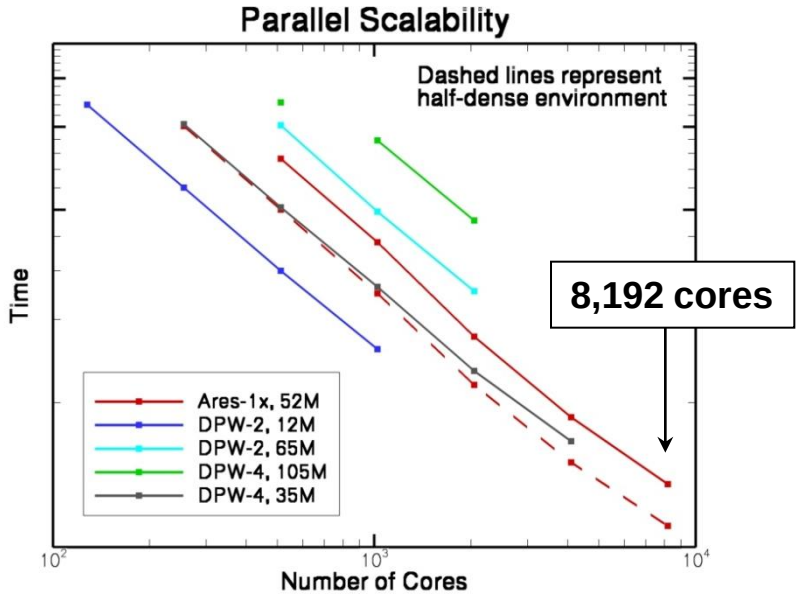

Parallel Grid/Solution Processing

Traditional Approach

- Most unstructured grid packages use a serial pre/post-processing paradigm
  - Separate step or,
  - Performed on the master node of the solver then broadcasted
- Very simple to implement, but does not scale:
  - 105M-node DPW-4 grid required 2 weeks, 800 GB of shared memory to preprocess for 1,024 cores using this approach

Users have neither the time nor hardware for this

Parallel Grid/Solution Processing

New Approach

- After several years of implementation, new fully-scalable paradigm now undergoing internal beta-testing
- Approach is fully distributed, requires no globally-dimensioned memory
- Raw grid loaded directly, processed in parallel, flows directly in-core to solver
- Solution restarts incorporate parallel I/O using MPI-IO layer
  - Leveraging Argonne research using FUN3D
- Solution visualization output now done at runtime using parallel co-processing
- Wide range of issues encountered
  - *Tremendous* challenge to write code w/o global indices: requires mappings, binary searches, bitwise operations, etc.
  - Traditional record-based file formats not amenable to extremely large grid sizes
    - File buffers require considerable memory overhead, often do not release all memory after I/O
    - Segmented records required to avoid record-length limitations; segment size may not align with data requirements
    - Very inefficient parsing
    - Stream-based I/O overcomes these issues – place file pointer directly at desired byte location: reduces I/O time by 50%, logic vastly easier, no unrecoverable memory
  - MPI-IO is standard in MPI-2, but some implementations still lack some functionality
- Enables user to perform routine analysis using $O(10^9)$-element grids (and larger) on commodity hardware

*105M-node DPW-4 grid now loaded, processed, and time-stepping initiated in **5 minutes** on 1,024 distributed cores*

Grid Adaptation

Local error based

- Feature based adaptation
- Flow solver/physics agnostic
- Not as robust
- Requires more manual interaction

Output error based

- Requires adjoint solution
- More robust
  - Transport of errors
- Fewer user controlled parameters

Output-Based Adaptation

- Mathematically rigorous approach involving the adjoint solution that reduces estimated error in an engineering output
- Uniformly reducing discretization error is not ideal from an engineering standpoint - some errors are more important to outputs

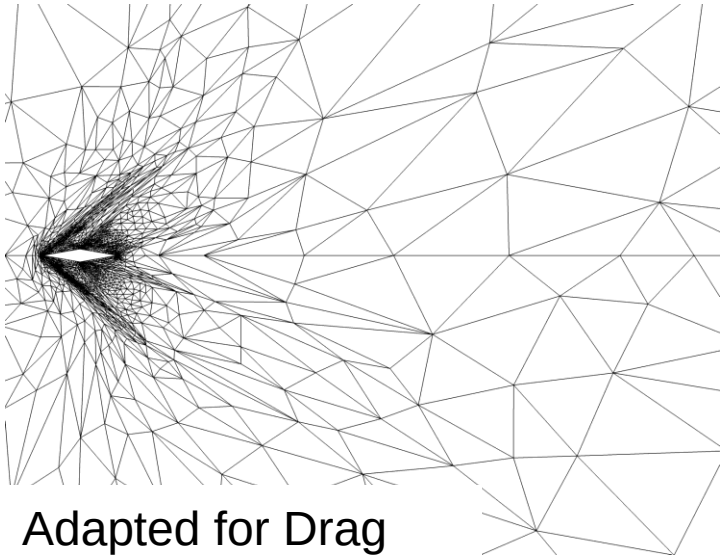

Adapted for Drag

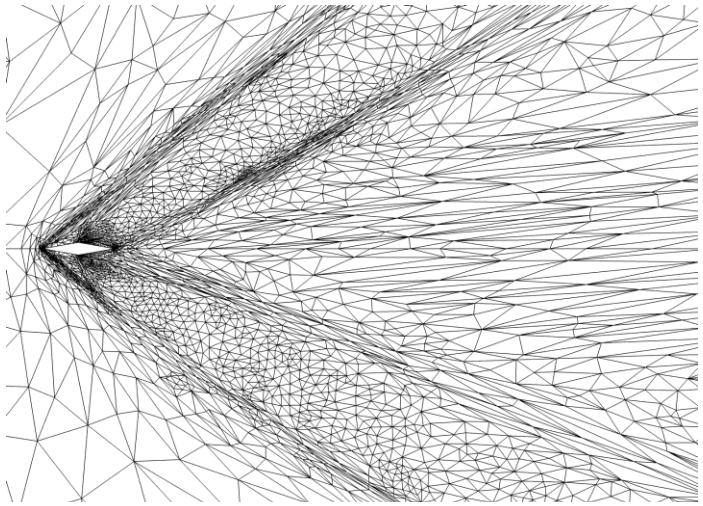

Adapted for Shock Propagation

NASA Langley Effort in Grid Adaptation

- Pioneering 3D anisotropic output-based adaptation for turbulent (RANS) simulation
- Utilizing the FUN3D framework to impact a large range of applications

Highly Anisotropic Adaptation

- Mapped isotropic methods produce large face angles
  - Discretization issues for gradient reconstruction
  - Mechanics unable to satisfy resolution request with face angle limits
  - *Circumvented with hybrid methods*
- Boundary recovery becomes increasingly difficult
  - *Circumvented with cut cells*

Sonic Boom Application-1

- Output-based adaptation has increased the automation of shock propagation simulations
- Euler delta wing body example (M = 1.68)
- Off-body pressure integral output

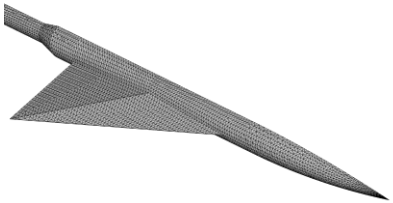

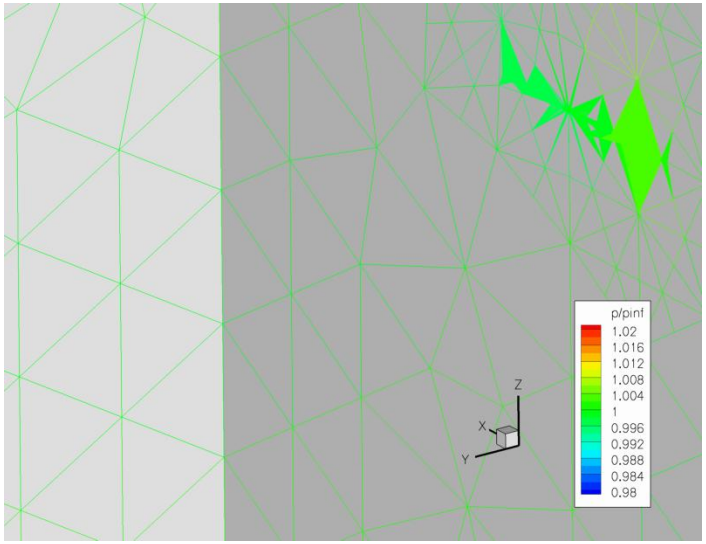

Initial Grid
2,800
Control volumes

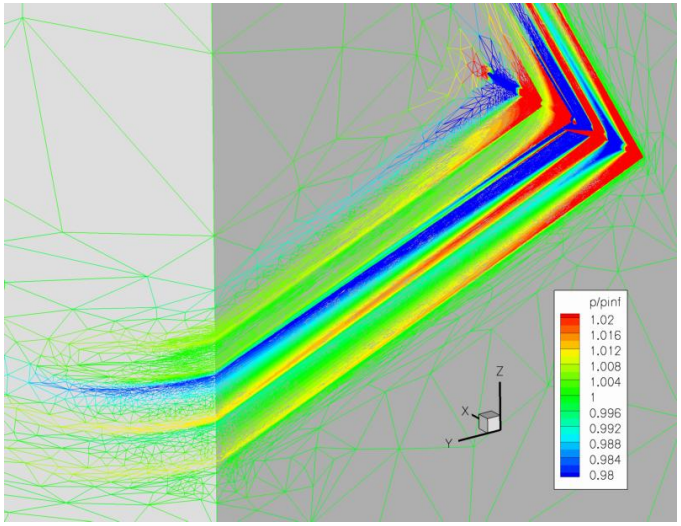

Final Adapted Grid
4,900,000
Control volumes

Sonic Boom Application-2

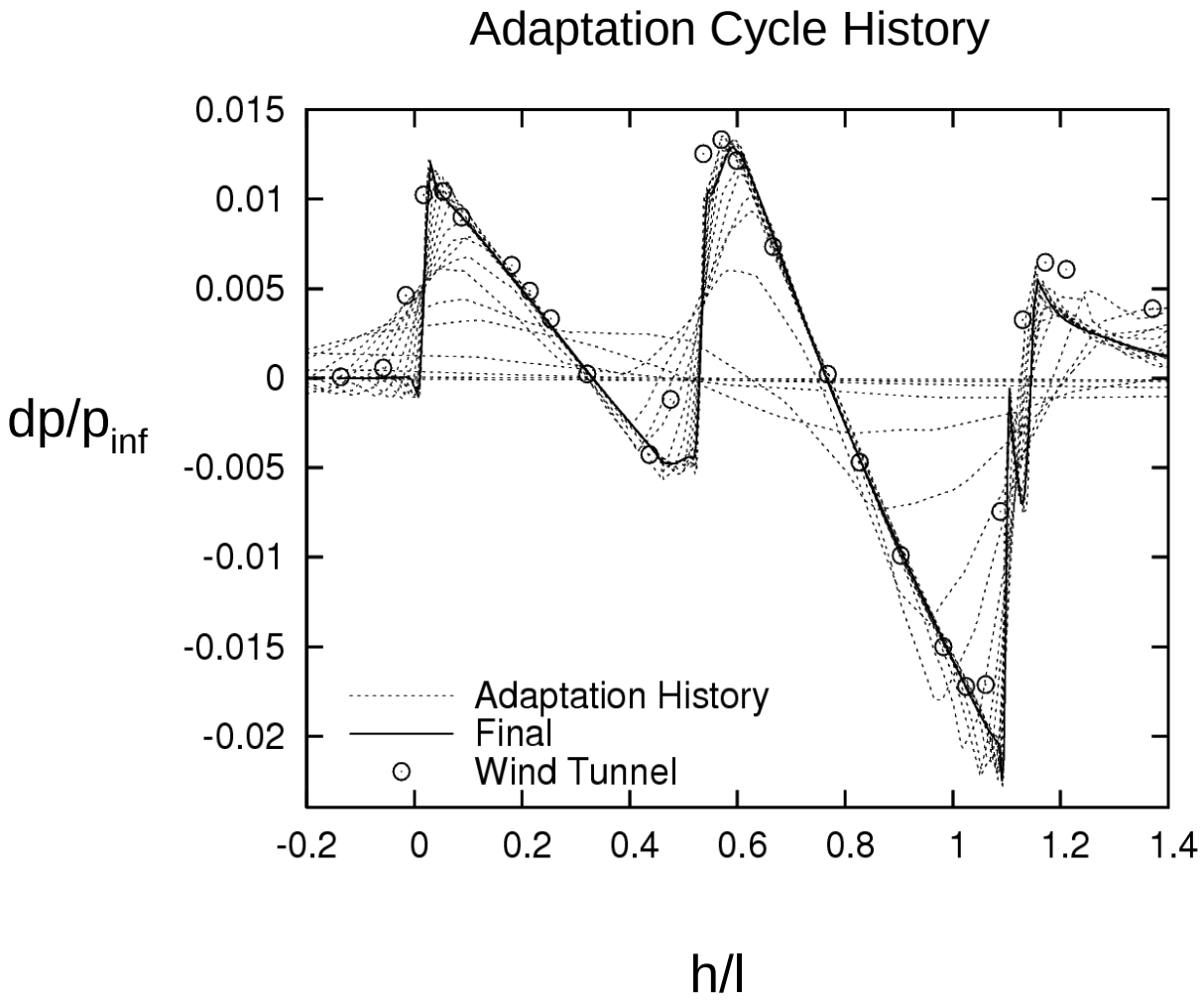

Adaptation For Viscous Flows

- Cut cell method for viscous flows
  - Work in progress
- Interim hybrid approach: freeze near-body high aspect ratio and surface curvature regions of body-fitted grids
  - Applicable to off-body features, but requires manual specification and generation of boundary layers
  - Particularly useful for capturing shear-layers, plumes, etc.

M = 2.25
8 deg wedge angle
PIV results available
Target: Drag

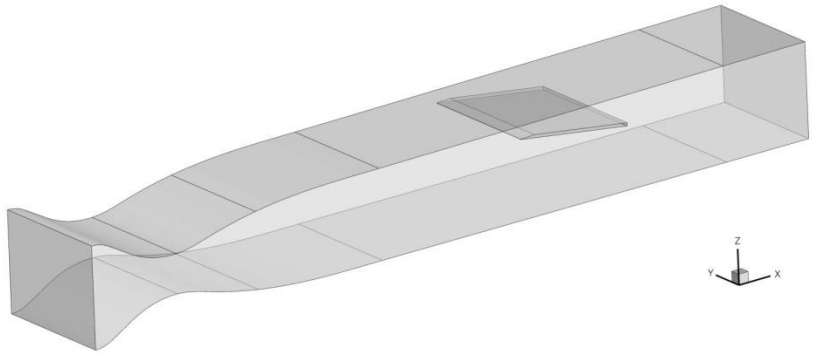

AIAA Shock/BL Interaction Workshop Problem

AIAA SBLI Workshop Problem-1

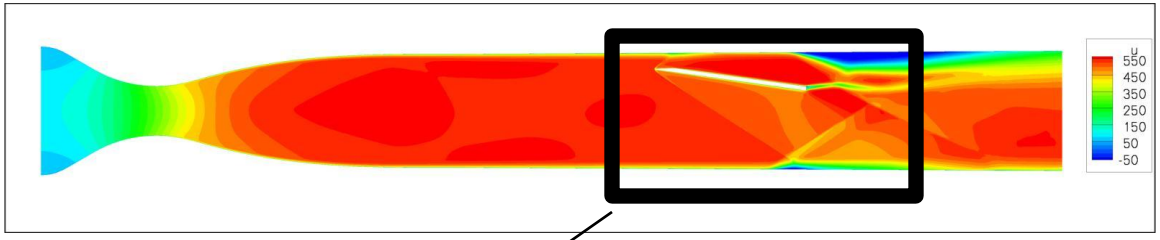

Original Grid

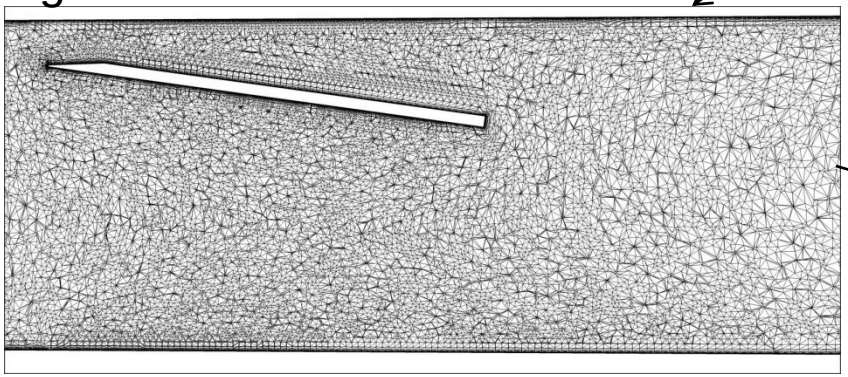

Adapted Grid

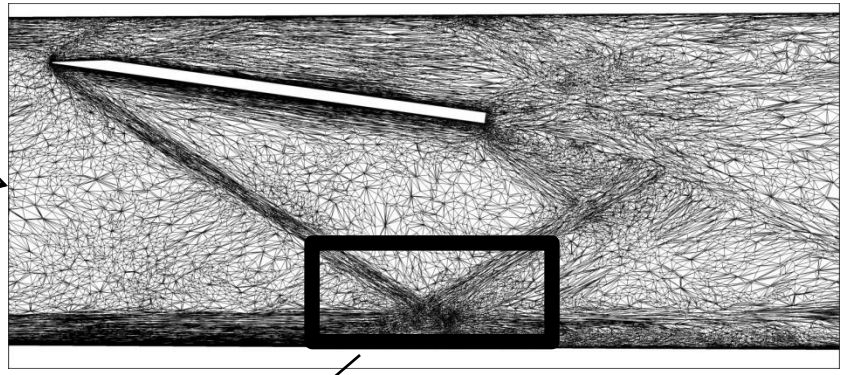

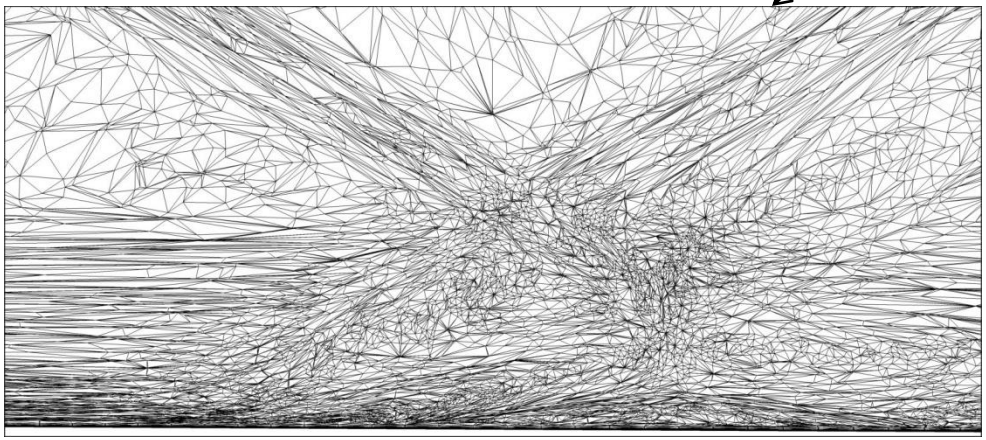

AIAA SBLI Workshop Problem-2

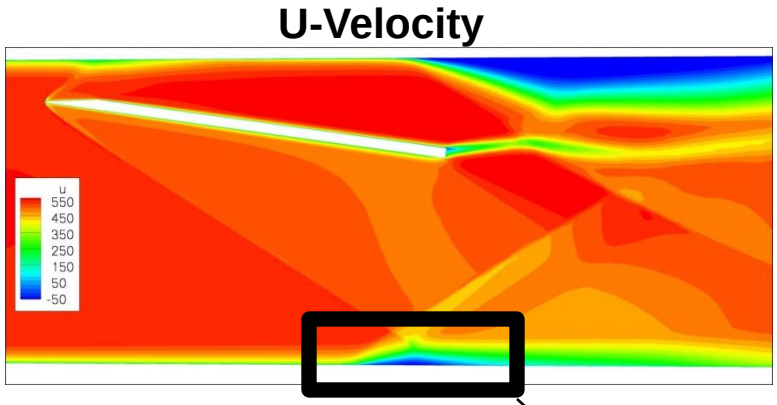

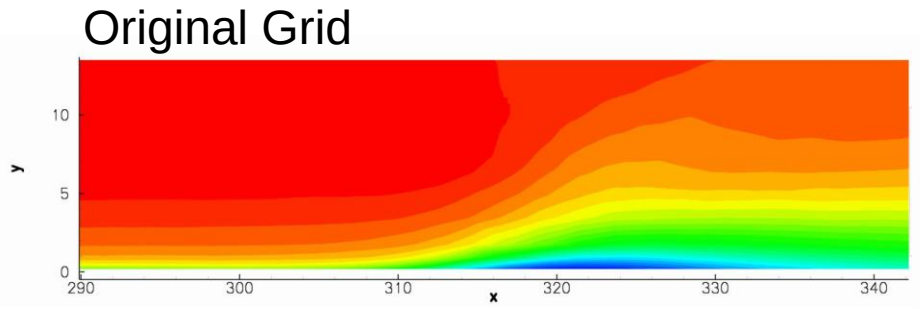

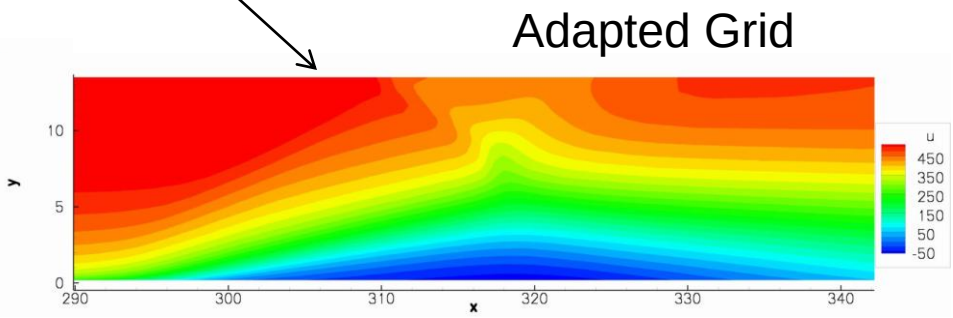

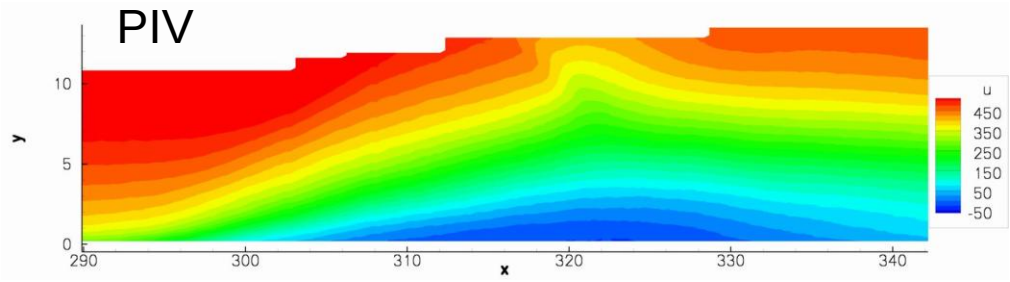

Motivation

- Conclusive code-verification for large-scale 3-D applications is beyond current capability (grids, computer time)
  - Drag Prediction Workshops I-IV illustrate difficulty
  - No nominally exact solution
  - Reliance on relative errors between codes and experiments

Transonic Wing-Body
Surface Flow

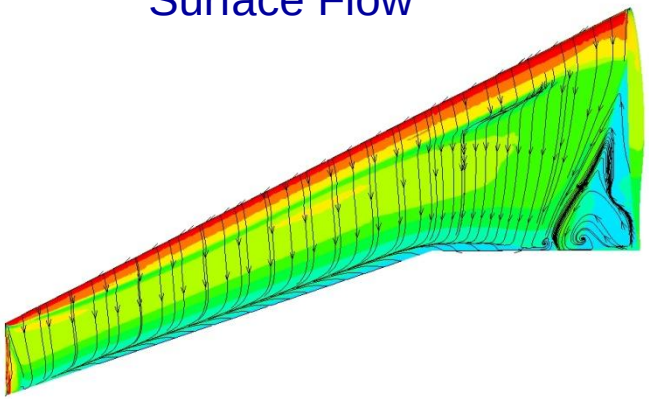

- Need to “bridge the gap”

- Verification possible in simpler settings
  - Problem features (e.g., flat plates)
  - Solution features (e.g., non-separated flow)
  - Grid features (e.g., regular refinement)

Inviscid Cylinder
Pressure Contours

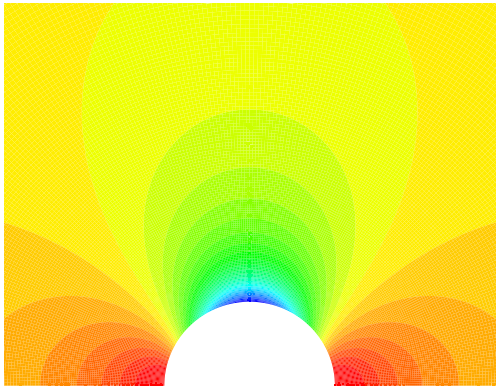

Outline
Remainder of Talk

- Code verification methodology
- Finite-volume discretizations
  - Node centered
  - Cell centered
- Grids
- Accuracy
  - Gradients
  - Viscous equations
  - Inviscid equations
- Agglomeration multigrid
- Summary

Summary CC and NC Schemes
Diffusion (Viscous Fluxes)

Standard NC scheme (Green-Gauss/Galerkin) is very attractive

- Low complexity
- 2^{nd} order discretization and remarkably insensitive to grid irregularities

Standard CC scheme (node-averaging) has serious drawbacks

- May degenerate on mixed grids
- High complexity
- Can fail to converge to the exact solution when clipping of node-averaged values is used

Alternative CC scheme (least-squares)

- Complexity similar to the NC scheme
- For accuracy and robustness, requires approximate mapping or stencil adaptation to reflect the direction of strong anisotropy

Accuracy and complexity per degree of freedom of the NC and the best CC schemes are comparable

Summary CC and NC Schemes
Convection (Inviscid Fluxes)

- Ordering of complexity (stencil size)
  - CC-LSQ (lowest)
  - NC
  - CC-NA scheme (highest)
- Current tests do not discriminate enough in accuracy
  - Large gradient errors are possible, but do not necessarily imply inaccurate solutions
  - All 2nd order schemes have similar discretization errors per degree of freedom
- Tests on grids of Class 3 (high aspect-ratio curved) are most discriminating for the NC path
  - Approximate-mapping and weighted-LSQ schemes provide accurate gradients
  - Weighted-LSQ schemes shown to be unstable in defect-correction
  - Approximate-mapped schemes are stable in defect-correction

Incorporating Improvement
Node-Centered FUN3D

- Baseline FUN3D reconstruction done with unweighted least-squares gradients even though inaccuracy known
- More than a decade of successful steady and time-dependent applications to complex geometries, including adaptation
- Mixed-element solutions required reconstructions with κ weighted toward central-difference for stability
- Approximate mapped least squares implemented
  - Little sensitivity of stability with κ
  - Initial assessments for transonic, rotorcraft, and hypersonic applications are very promising

Cell Centered (CC) vs Node Centered (NC)

- Compared in controlled environment
  - Method of manufactured solutions
  - Consistently refined (irregular) grids
  - The same type of boundary conditions
- Systematic studies
  - Gradients in NIA Report 2008-12
  - Viscous (pure diffusion) in AIAA 2009-597
  - Convection in AIAA 2010-1079
  - Reynolds Averaged Navier-Stokes ongoing

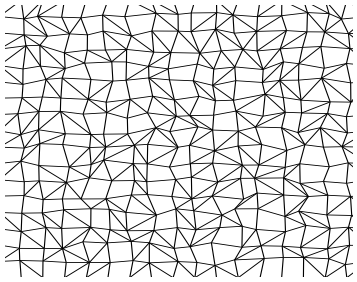

Isotropic

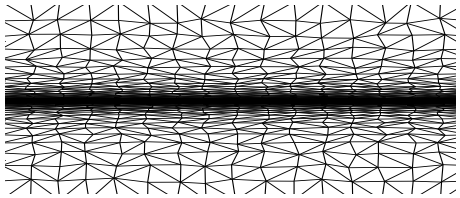

High AR

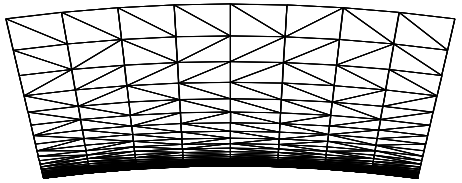

High AR + Curvature

Which is the Better Grid?

High AR

Small perturbation in y (Family 1)

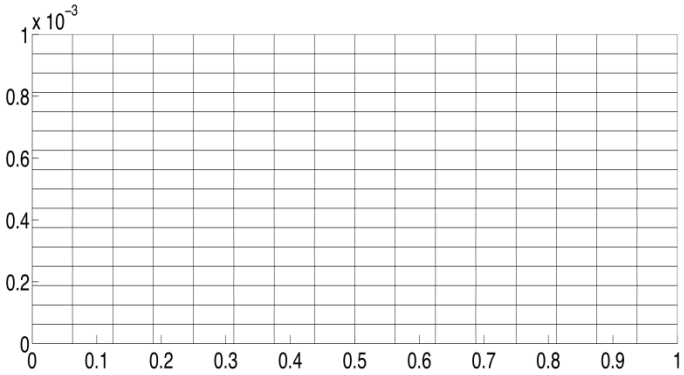

Noticeable perturbation in x (Family 2)

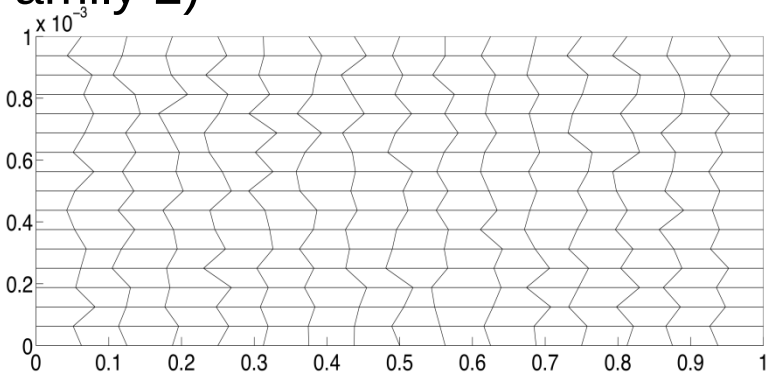

The correct answer is scheme-dependent. For the node-centered weighted least-square scheme, Family 2 is better – Family 1 is nonconvergent.

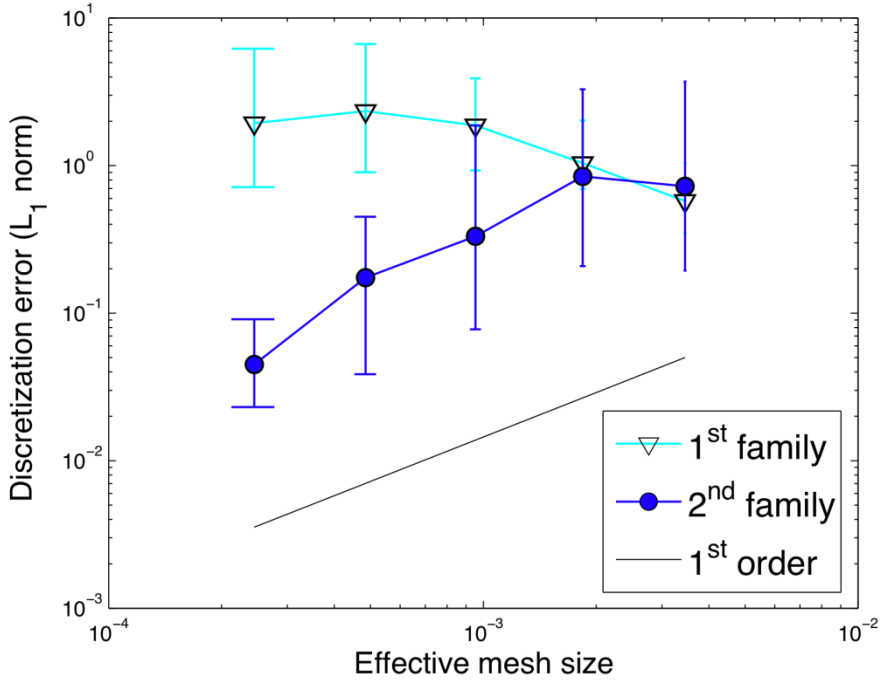

Summary
Comparison of CC and NC Schemes

NC and the best CC schemes are comparable

- •Gradient accuracy deteriorates on high-aspect-ratio regions on irregular grids
- •Improved accuracy in high-aspect-ratio curved grids with approximate mapping techniques
- •Identified serious drawbacks of several existing schemes

Developed promising alternative CC scheme (least-squares)

- • Lower complexity than existing schemes
- • Equivalent accuracy

Agglomeration Multigrid-1

- Agglomeration multigrid method follows pioneering work of Venkatakrishnan and Mavriplis with modifications
  - Topology-preserving agglomerations
  - Consistent coarse-grid discretization
- Both cell-centered and node-centered discretizations

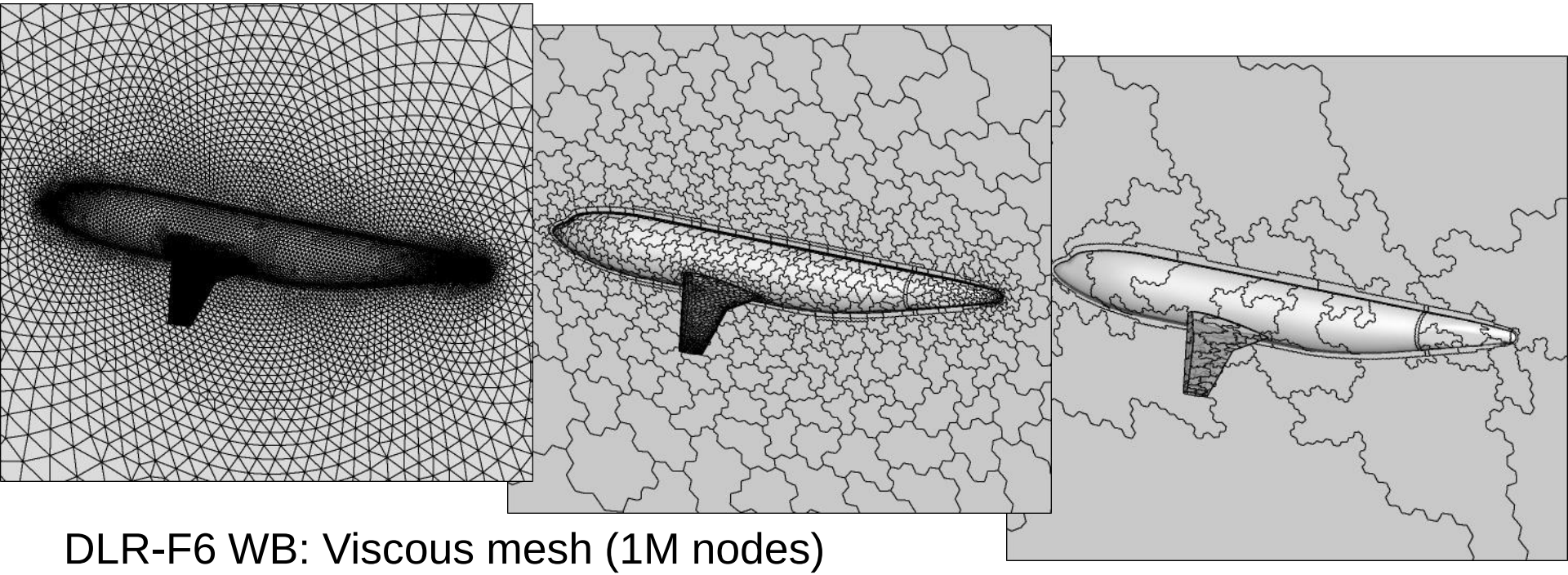

DLR-F6 WB: Viscous mesh (1M nodes)

Agglomeration Multigrid-2

- Diffusion on isotropic grids (AIAA-2009-4138/AIAA J)
  - Showed grid dependence with inconsistent coarse grids
  - Applied quantitative multigrid analysis tools
    - Ideal Coarse Grid (ICG)
    - Ideal Relaxation (IR)
- Diffusion on highly stretched grids (Computers & Fluids 2010)
  - Developed IR operator for line relaxation
  - Showed limitations with tetrahedral grids both theoretically and practically
  - Grid-independent convergence with full coarsening and line relaxation with prismatic cells in highly stretched regions
- Euler and RANS for complex geometries ongoing (AIAA paper Summer 2010)

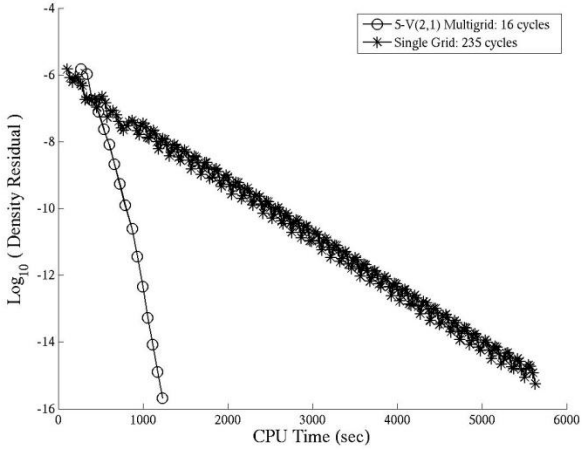

Inviscid results (1M nodes): ~6 times faster, including the time to generate coarse grids.

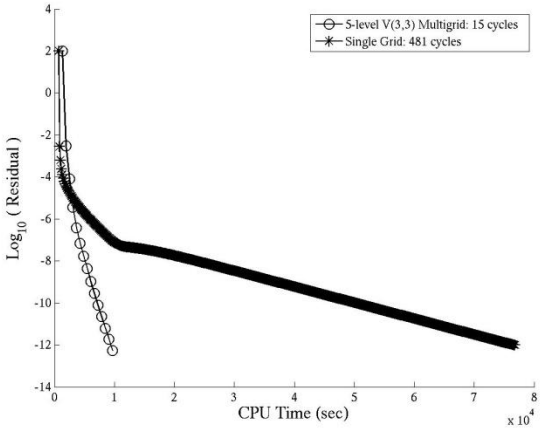

DPW-W2(1.9M nodes); Diffusion equation.

Grid-Independent Convergence

Diffusion ; $(A)_{max}$=1000

Primal Mixed-Element Grid

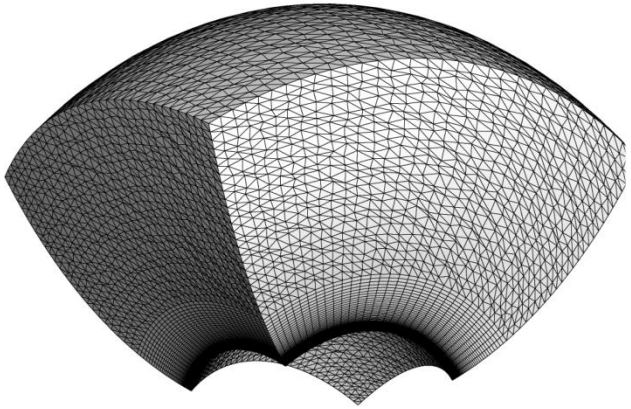

1st Agglomerate

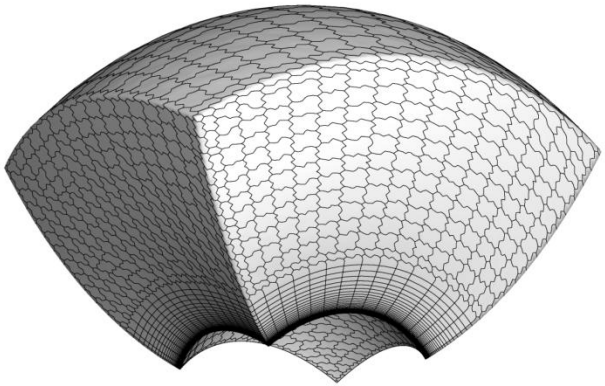

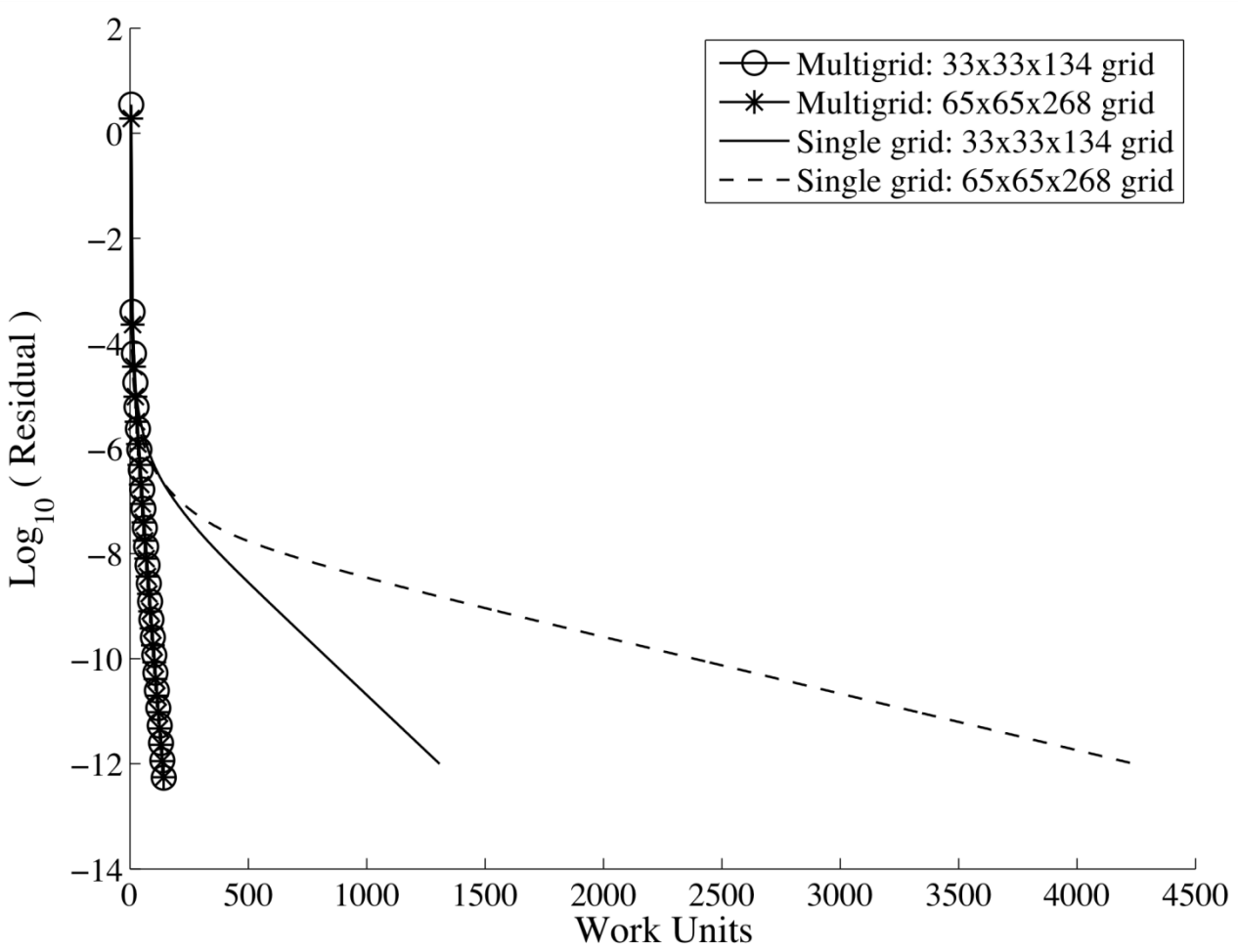

Agglomeration Multigrid

Towards grid-independent convergence for fully unstructured grids

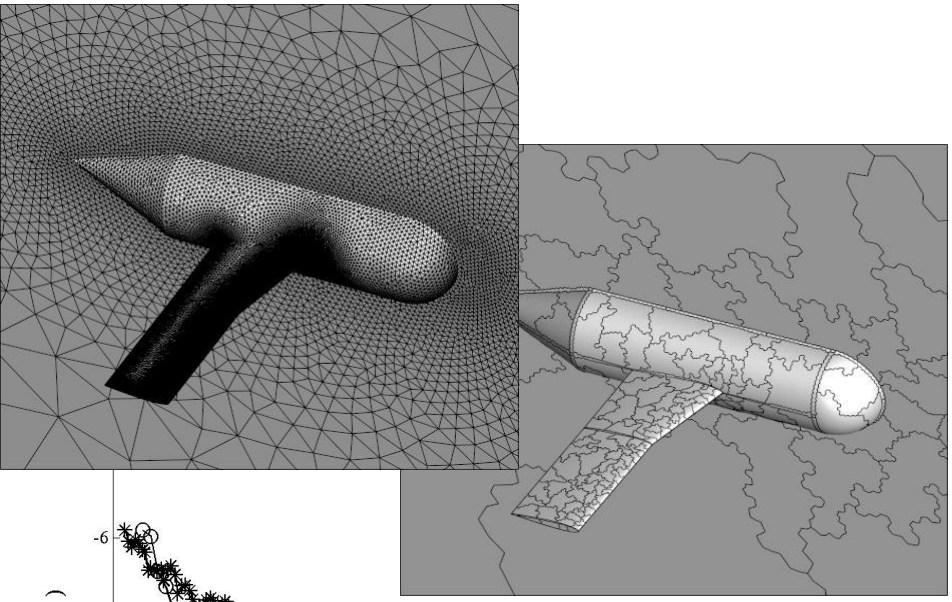

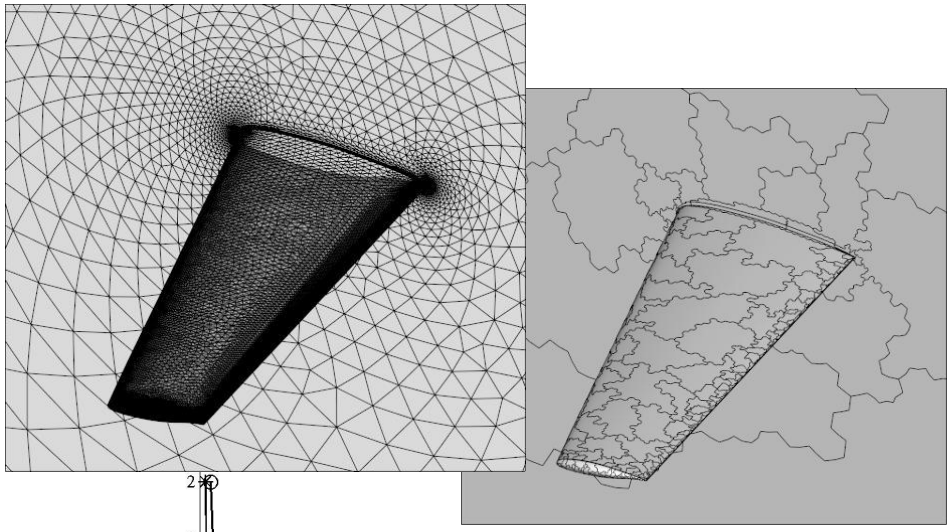

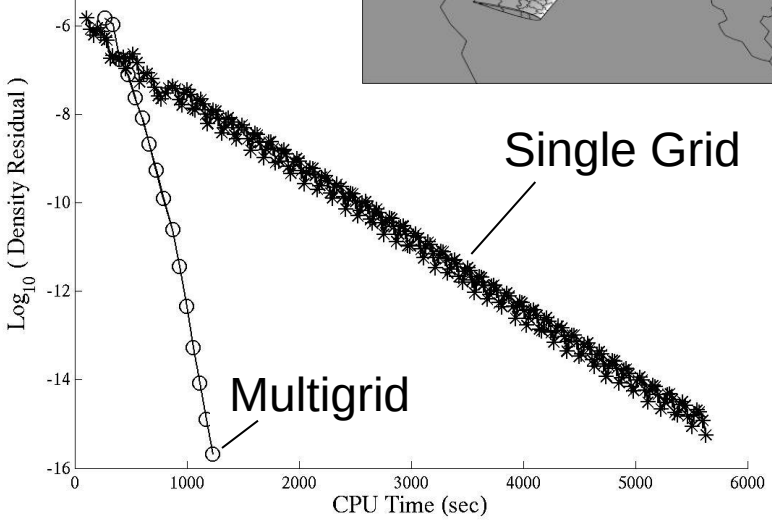

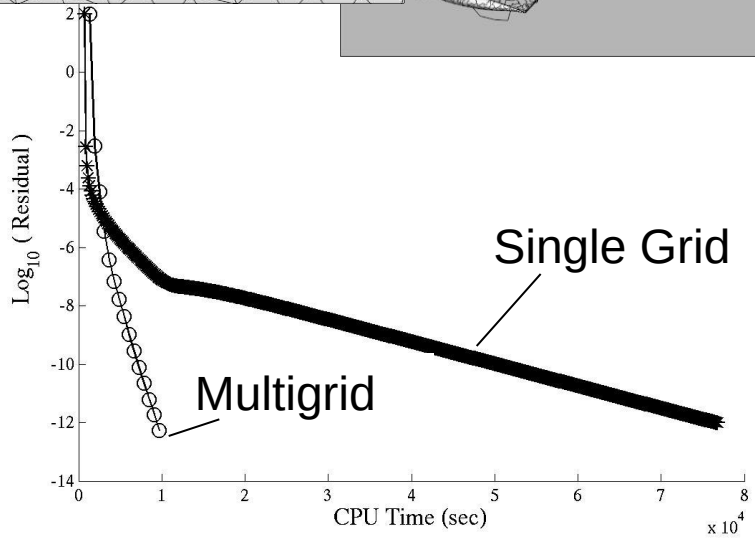

Inviscid results (1M nodes): ~6 times faster, including the time to generate coarse grids.

DPW-W2(1.9M nodes); Diffusion equation.

Summary

Developments

- Improved discretizations through identification and isolation of difficulties
- Improved agglomeration multigrid method using quantitative analysis tools

Ongoing Work

- Assess solvers for turbulent equations as model emphasizing strong source terms and importance of gradient accuracy
- Extend agglomeration multigrid method to time-dependent RANS

FUN3D - Tetrahedral Grids

- **Develop algorithm to enable accurate simulation of heating and shear in hypersonic flow simulations on tetrahedral grids**
  - Tetrahedral grids provide greatest flexibility for adaptation
    - Complex Geometries/Flows
    - Flexible Ballute
    - Retro-Propulsion
  - BUT… Exclusive use of tetrahedral grids in finite-volume formulations yields poor simulation of heating - especially in stagnation region.

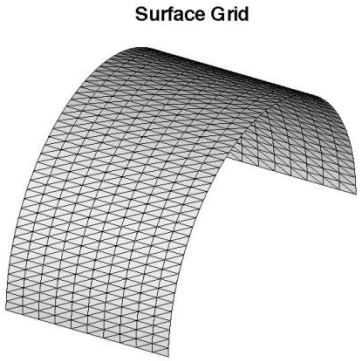

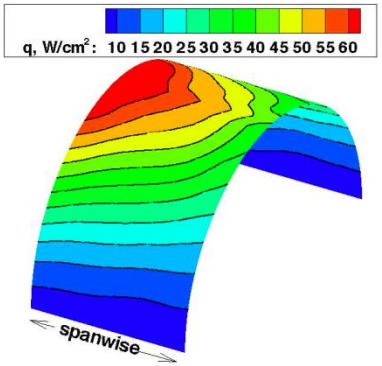

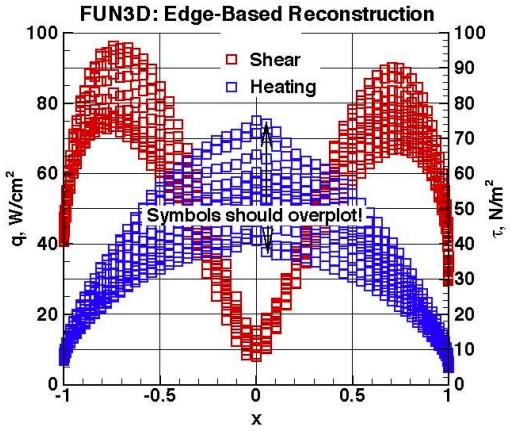

Mach 17, 2D Flow Over a Cylinder

One Dimensional, Edge Based Reconstruction

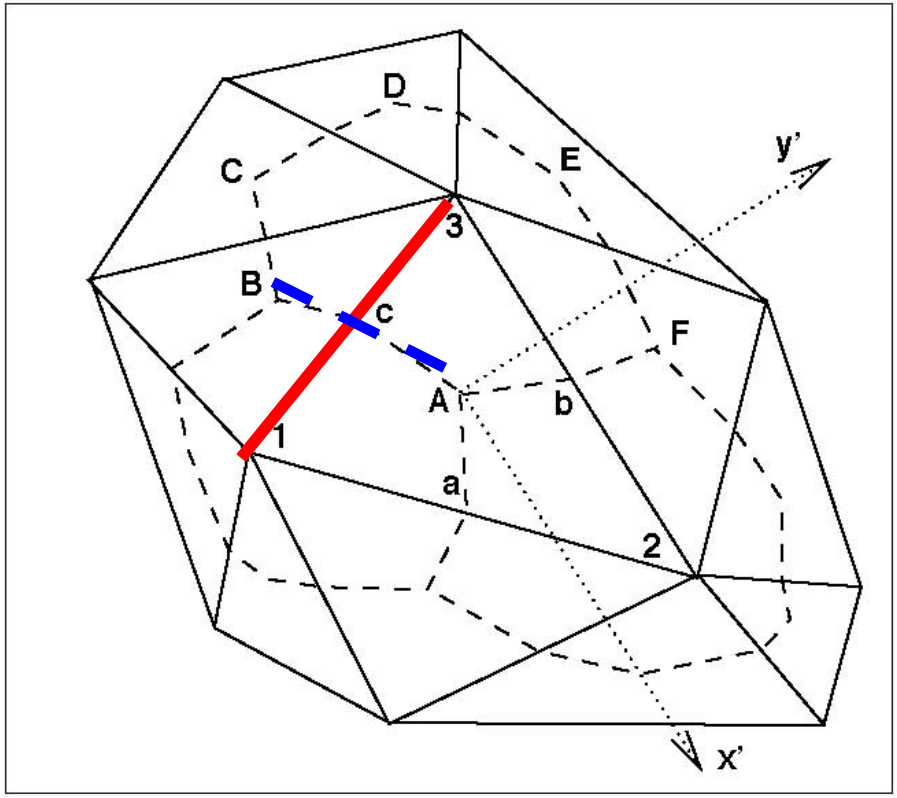

Loop over edges (red)

Compute flux f_c across single face separating two nodes (blue)

$$f_c(q_1, q_3, \nabla q_1, \nabla q_3)$$

Three-Dimensional, Element Based Reconstruction

Loop over elements (magenta)

Compute flux f_{cAa}, f_{cAb}, and f_{bAa} for the three faces (blue) separating the three nodes defining the element

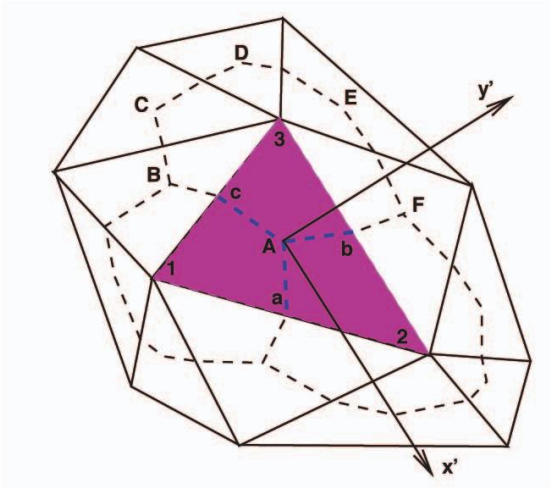

Central Idea *(Peter Gnoffo)*

- Placing stronger emphasis on flow topology for definition of inviscid flux (and less emphasis on edge orientation) is expected to improve simulation accuracy.

$$f_{cAa} = f_{x'} n_{cAa,x'} + f_{y'} n_{cAa,y'}$$

$$f_{cAb} = f_{x'} n_{cAb,x'} + f_{y'} n_{cAb,y'}$$

$$f_{bAa} = f_{x'} n_{bAa,x'} + f_{y'} n_{bAa,y'}$$

$$f_{x'}(q_{R,x'}, q_{L,x'}, \nabla q_{R,x'}, \nabla q_{L,x'})$$

$$f_{y'}(q_{R,y'}, q_{L,y'}, \nabla q_{R,y'}, \nabla q_{L,y'})$$

The metrics used here are identical to those already used in the viscous flux formulation.

Mach 17 Challenge Problem Revisited

Original

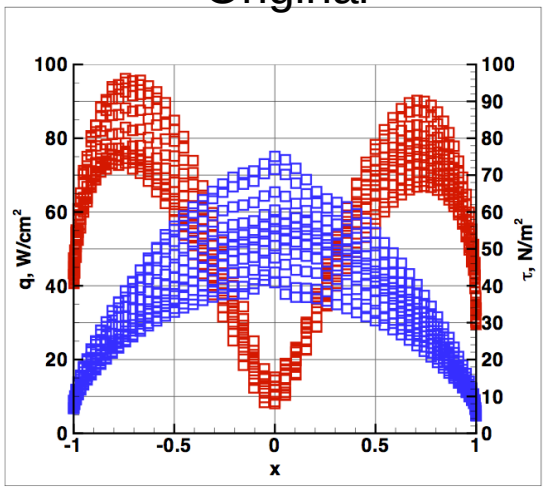

11 spanwise nodes

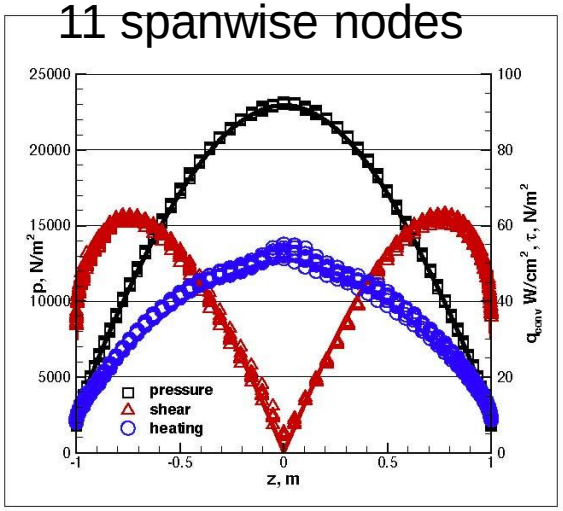

7 interior nodes

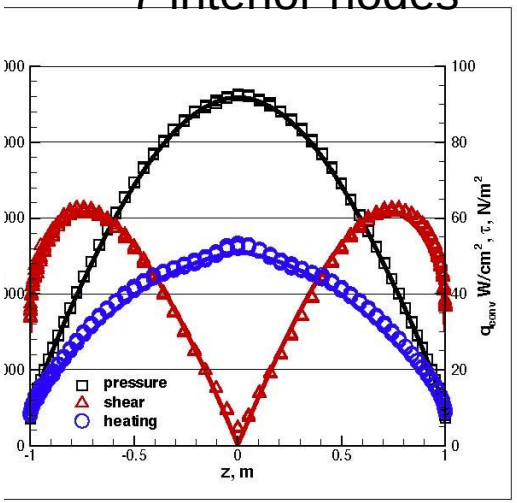

heating

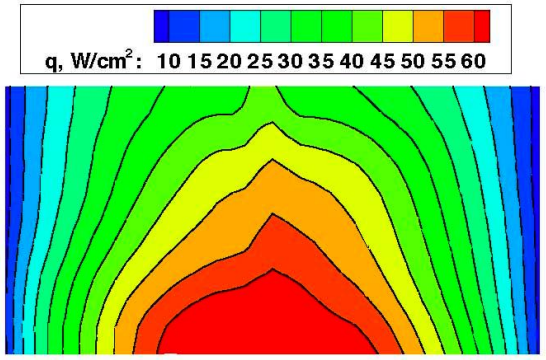

heating

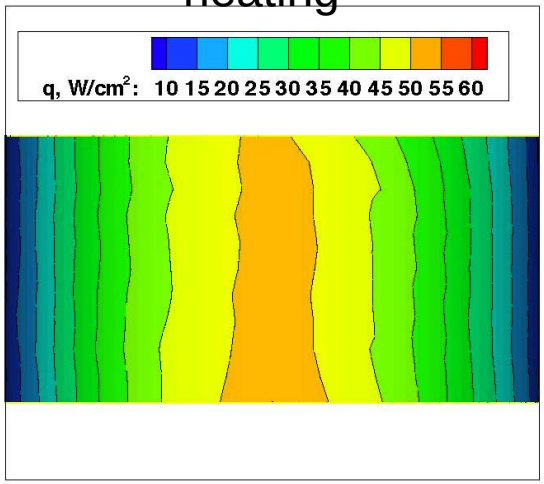

shear

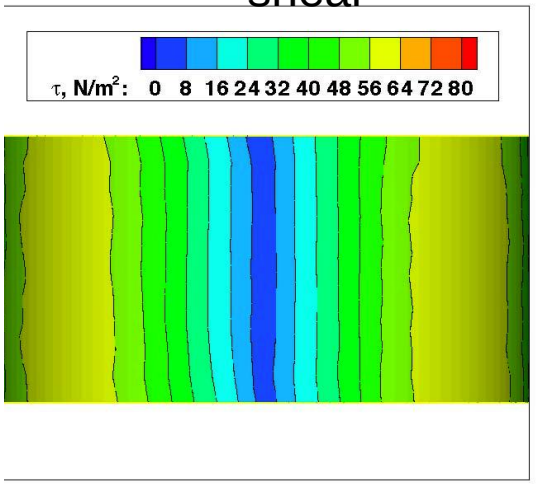

Another Challenge Problem: Mach 12 Flow over a Sphere

Hex Grid

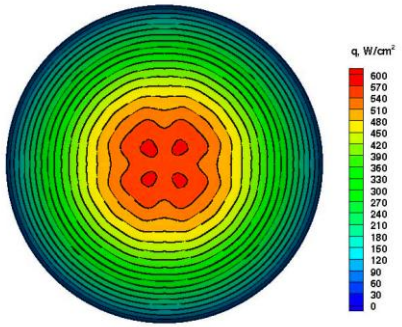

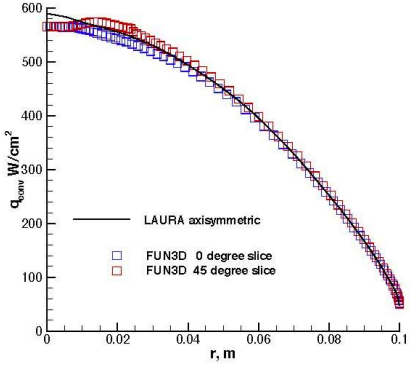

Tet Grid - 1D Reconstruction

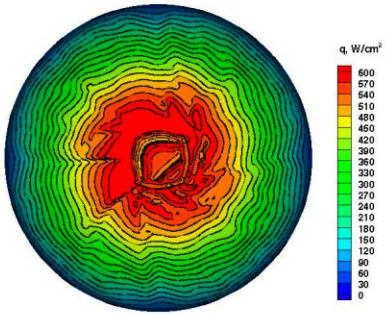

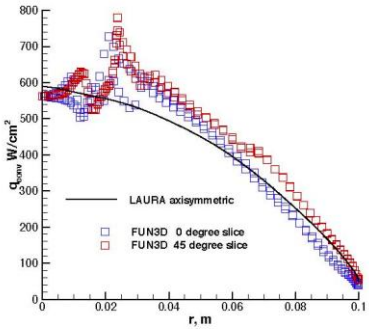

Tet Grid - 3D Reconstruction

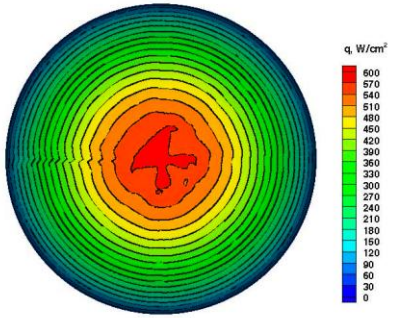

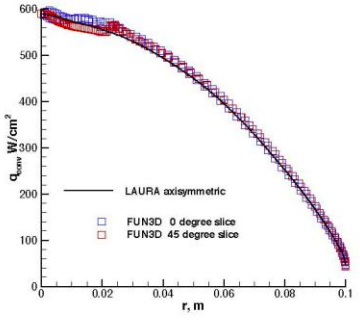

Design Optimization Using FUN3D

- Long history of adjoint-based methods for steady flows
- Discretely consistent implementation for full 3D RANS
- Design framework based on high-level wrappers to perform analysis and sensitivity analysis using FUN3D executables
  - Provide interface support for PORT, NPSOL, KSOPT libraries
  - New optimization packages largely plug-n-play
- Two general classes of design variables for steady problems
  - Global parameters ($\mathbf{M}_\infty$, α, etc)
  - General shape parameterizations (MASSOUD or “bandaids” from LaRC, Sculptor, CAD via Capri, proprietary schemes, etc – user just provides $\mathbf{X}_{surf}$, $\partial\mathbf{X}_{surf}/\partial\mathbf{D}$ in specified file format)
- Unconstrained, constrained (penalties or explicit), multipoint, multiobjective
  - Provides as many functions and gradients as requested; only limited by optimization package being used

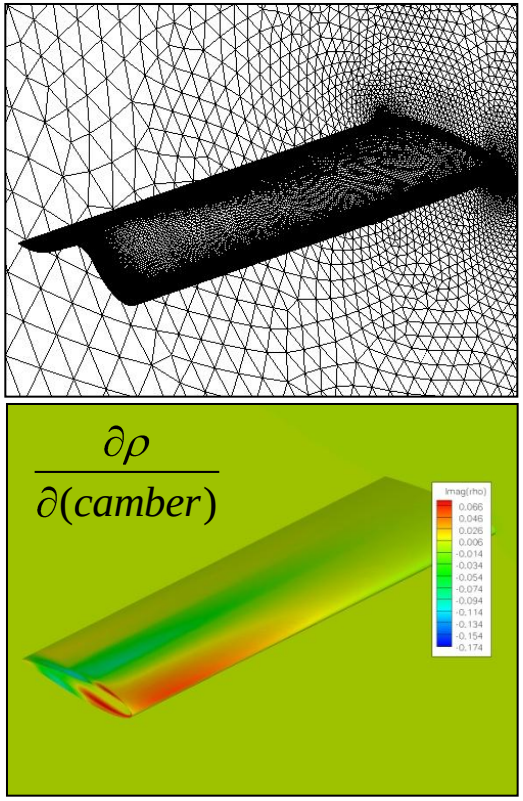

Imaginary part of solution shows sensitivity of surface loading

Derivation of the Time-Dependent Adjoint Equations

As in steady cases, construct Lagrangian using an objective function and adjoint variables multiplying the governing equations as constraints:

$f \equiv$ Objective function

$\boldsymbol{\Lambda}_f \equiv$ Flowfield adjoint variable $\quad \mathbf{R} \equiv$ Spatial residual

$\boldsymbol{\Lambda}_g \equiv$ Grid adjoint variable $\quad \mathbf{R}_{GCL} \equiv$ GCL residual

(BDF1 shown here for simplicity; higher order schemes also implemented)
(X = computational grid, D = design variable, GCL = geometric conservation law

$$L(\mathbf{D},\mathbf{Q},\mathbf{X},\boldsymbol{\Lambda}_f,\boldsymbol{\Lambda}_g) = \overbrace{\sum_{n=1}^{N} f^n \Delta t}^{\text{Objective Function}} + \sum_{n=1}^{N}\left[\boldsymbol{\Lambda}_f^n\right]^T \overbrace{\left(\mathbf{V}^n \frac{\mathbf{Q}^n - \mathbf{Q}^{n-1}}{\Delta t} + \mathbf{R}^n + \mathbf{R}_{GCL}^{\,n}\mathbf{Q}^{n-1}\right)\Delta t}^{\text{Flow Equations}}$$

$$+ \sum_{n=1}^{N}\left[\boldsymbol{\Lambda}_g^n\right]^T \underbrace{\mathbf{G}^n \Delta t}_{\text{Grid Equations}} + \underbrace{f^0 + \left[\boldsymbol{\Lambda}_f^0\right]^T \mathbf{R}^{in}\ \Delta t + \left[\boldsymbol{\Lambda}_g^0\right]^T \mathbf{G}^0 \Delta t}_{\text{Similar terms for initial conditions}}$$

- Linearize with respect to **D**, isolate the coefficients of $\partial\mathbf{Q}^n/\partial\mathbf{D}$ and $\partial\mathbf{X}^n/\partial\mathbf{D}$, and equate them to zero

General Unsteady Implementation

- Adjoint solution must be initiated at time level N and marched in reverse physical time: flow solution $\mathbf{Q}^n$ at all time levels must be available during reverse integration
- Current approach is to store $\mathbf{Q}^n$ to disk for all n; also store $\mathbf{X}^n$ and $\partial\mathbf{X}^n/\partial t$ for dynamic mesh cases (total of 12 variables/grid point)
  - Pro: Ease of implementation
  - Con: Significant storage cost – can easily yield disk requirement of $O(TB)$
- Simultaneously parsing hundreds of sequential-access files of several gigabytes each at each time step very inefficient; direct-access files reduce disk I/O time by two orders of magnitude
- Dual time-stepping used for the adjoint solution, similar to flow solution
- GCR scheme used to wrap multicolor Gauss-Seidel and temporal subiterations: stabilizes linearly unstable iterations occasionally encountered
- Infrastructure required to simultaneously manage/shuffle data from as many as 7 time levels: current + 3 forward + 3 reverse

Tiltrotor Example

- Geometry based on the three-blade Tilt Rotor Aeroacoustics Model (TRAM), similar to that used by the V-22
- Grid designed for Θ=14° blade collective setting; contains 5,048,727 nodes and 29,802,252 tetrahedral elements
- Rotational speed held constant such that M_{tip}=0.62 in hover, Re_{tip}=2.1 million
- Δt chosen according to 1° of rotor azimuth for 360 steps/rev
- $BDF2_{opt}$ used with 10 subiterations
- Rigid grid motion: 4 revs to quasi-steady hover condition, followed by 90° pitch-up maneuver with prescribed forward velocity over 5 additional revs

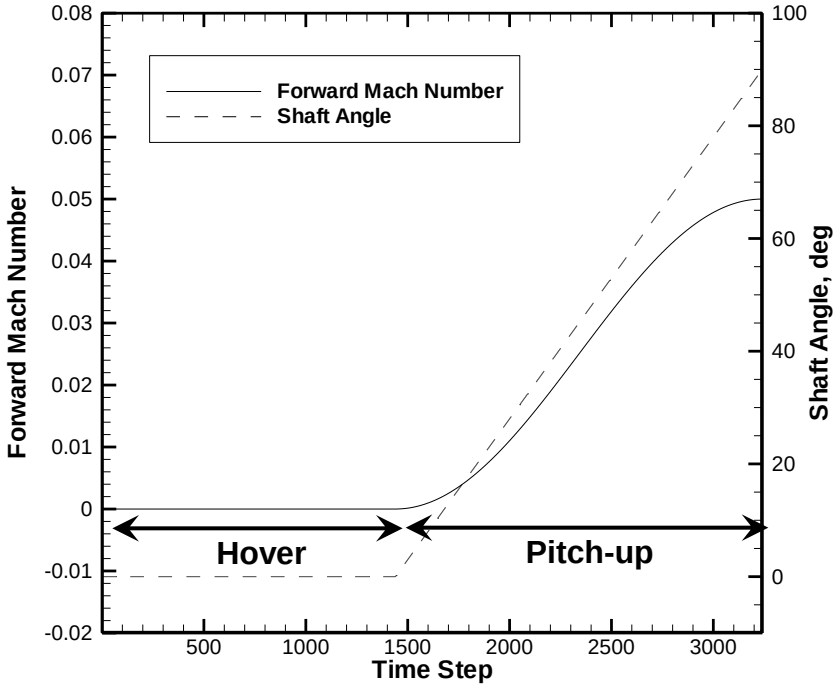

Tiltrotor Example

- Objective function is to maximize the thrust coefficient over the pitch-up maneuver:

$$f = \sum_{n=1441}^{3240} (C_T^n - 0.1)^2 \Delta t$$

- Blades parameterized as shown, no thinning allowed
- Blade twist also used to set the collective angle
- Total of 45 active design variables

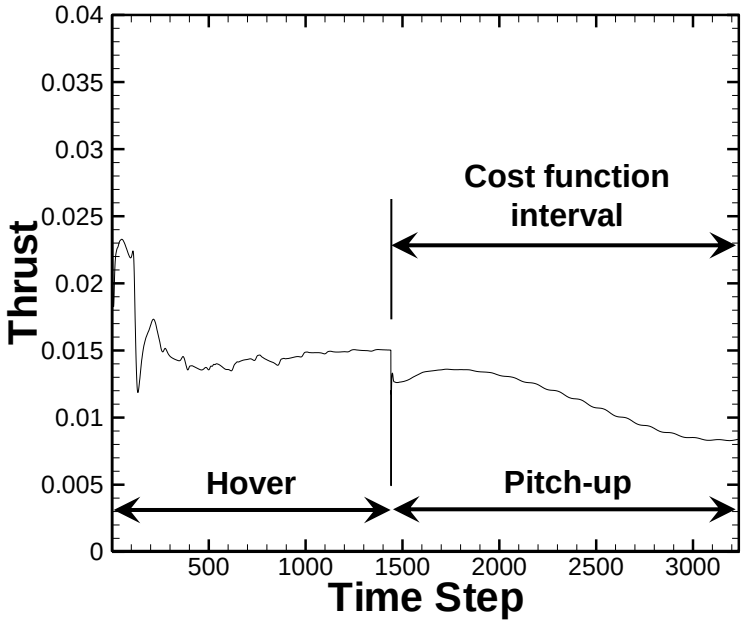

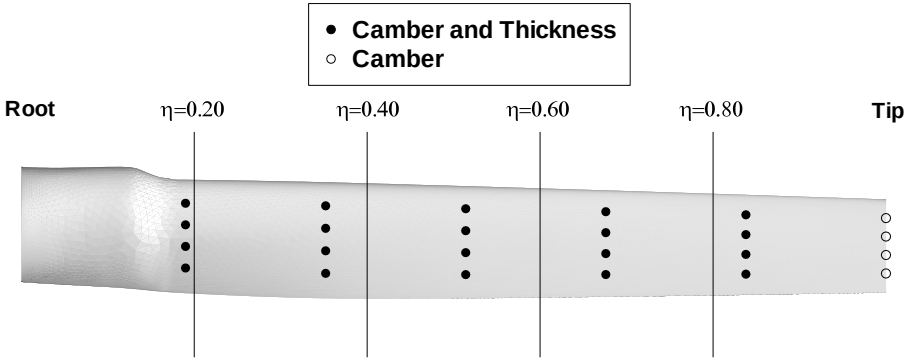

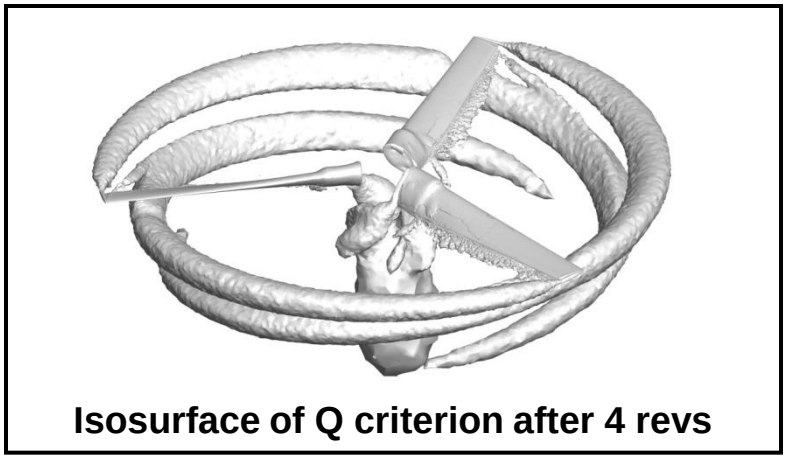

Tiltrotor Example

- Rapid reduction in cost function over first two design cycles; further improvements minimal
- Camber, collective angle have been increased across the blade; many variables have reached their bounds
- Single flow solution takes ~3.5 hours
- Single adjoint solution takes ~10.5 hours; varies w/ file system load due to heavy I/O
- Optimization requires 12 flow solutions and 6 adjoint solutions for total runtime of 4.5 days or 110,000 CPU hours
- Disk storage for single unsteady flow solution is 1.5 terabytes

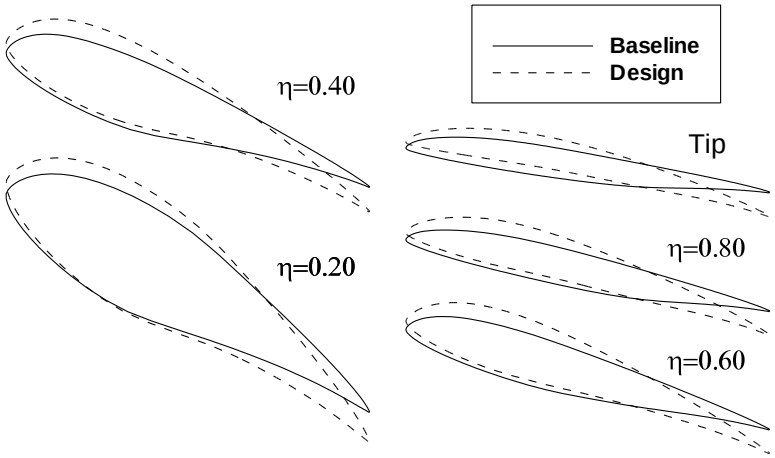

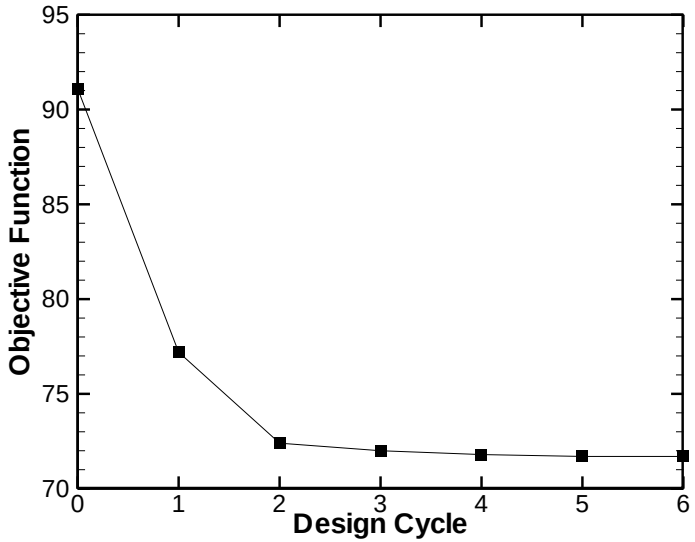

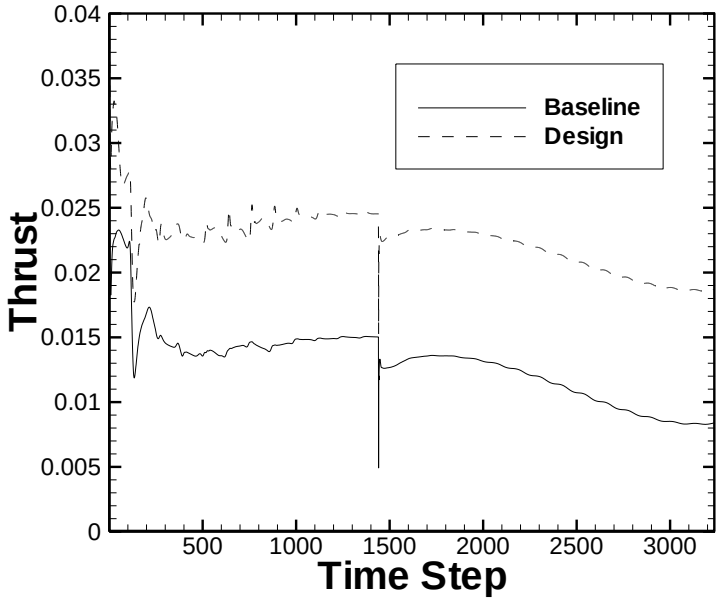

How Do We Compute the Noise?

Unsteady Numerical Simulation

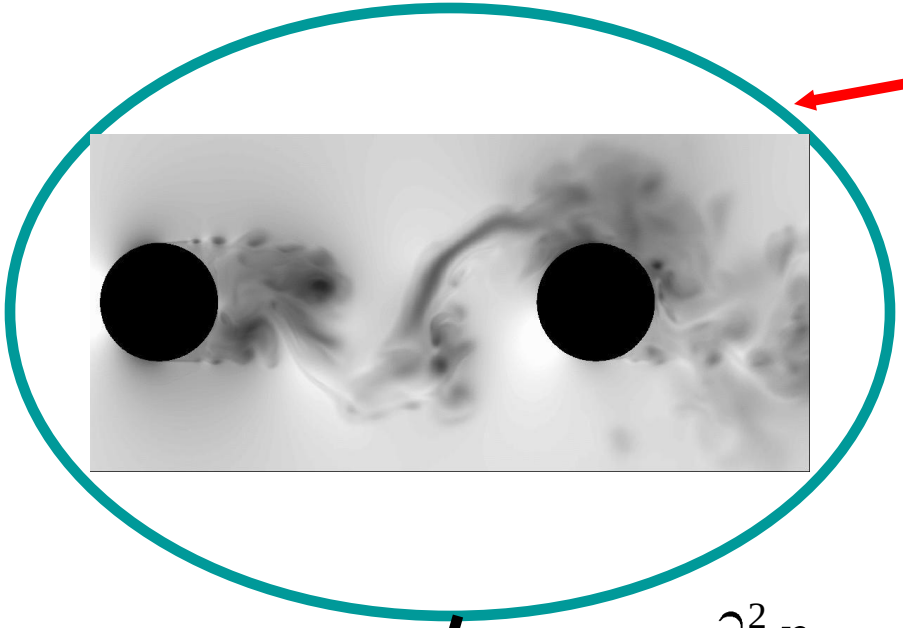

Accurately determine the unsteady noise source characteristics and account for near-field scattering.

$$\frac{\partial^2 p}{\partial t^2} - c_o^2 \frac{\partial^2 p}{\partial x_i \partial x_i} = \Box^2 p = S(x_i)$$

Experiment

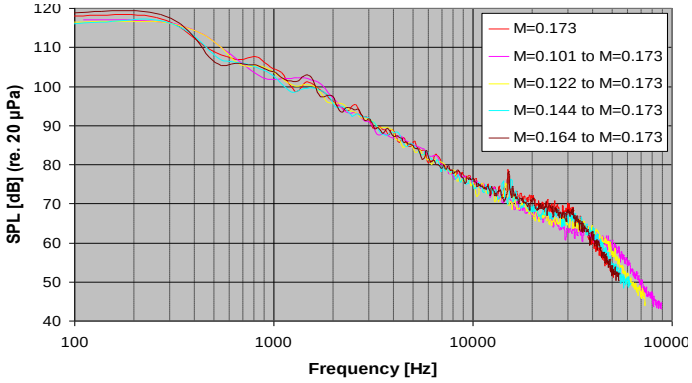

Obtain the noise at far-field listener positions

- **Physical insight**
- **Cause & effect relationships**
- **Detailed source description**

Computational Approach

- Unsteady CFL3D Computations
  - 3D Navier-Stokes solver
  - Upwind, nominally 2nd order in space
  - 2nd order implicit time stepping (dual time)
  - Modified Menter's SST K-ω turbulence model
    - Production term turned off outside of boundary layers

- Block Structured Grids
  - Spans of 3, 6, 18
  - Grid refinement
    - 5M – 80M grid points

- Operating Conditions
  - Re=166E3
    - Fully turbulent simulations
    - Transition strip used in experiments
  - M=0.166

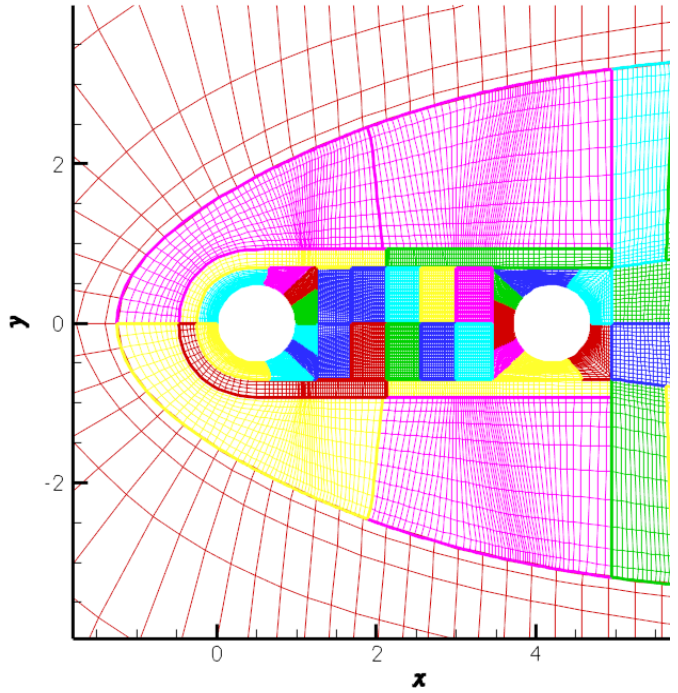

em Cylinders

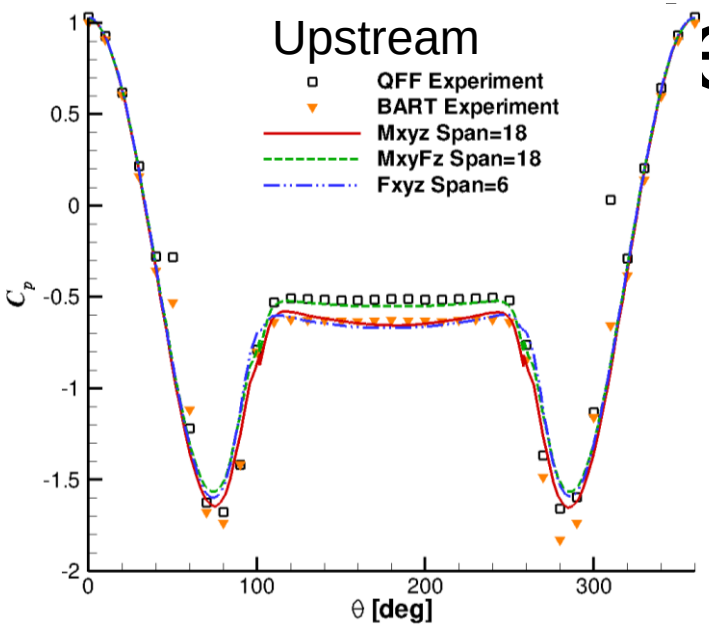

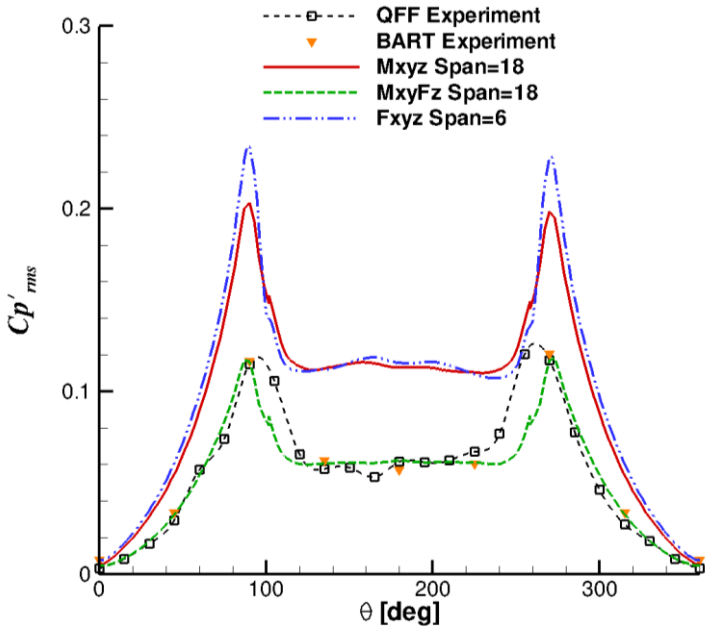

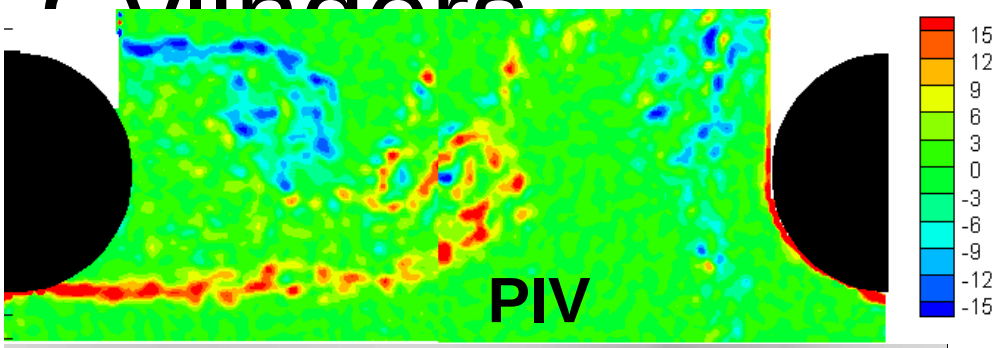

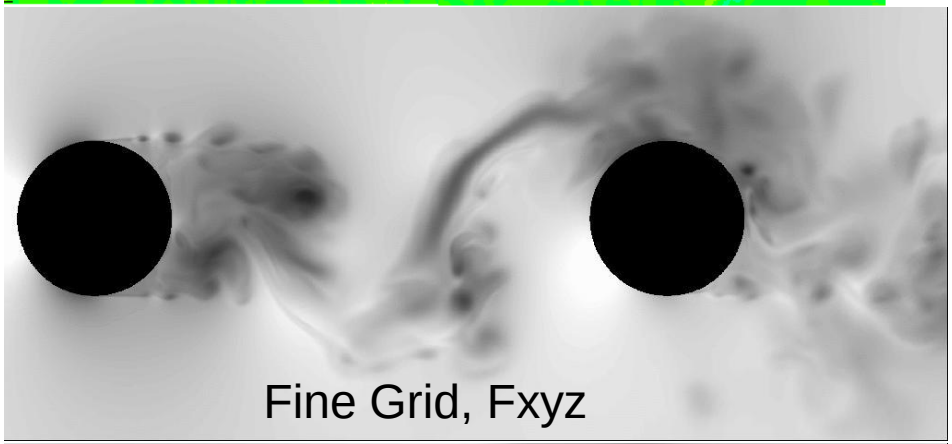

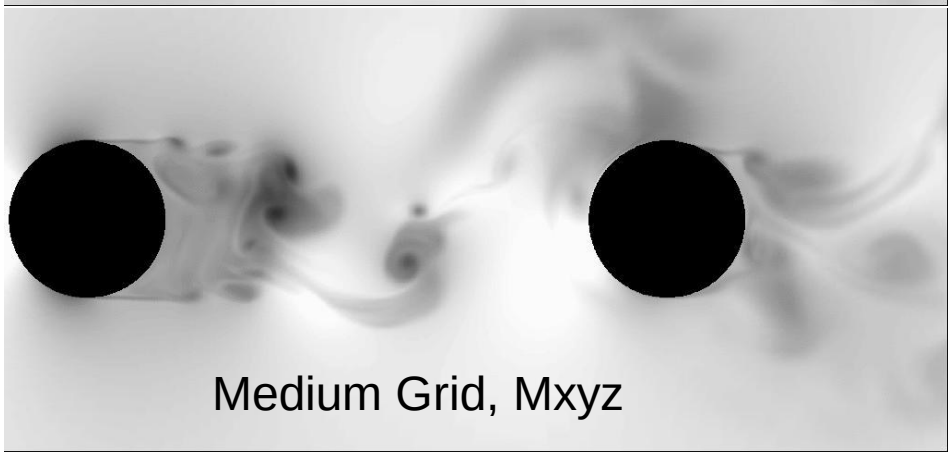

Computational Approach

- Ffowcs Williams – Hawkings Noise calculations
  - Integral technique derived from the Navier-Stokes equations

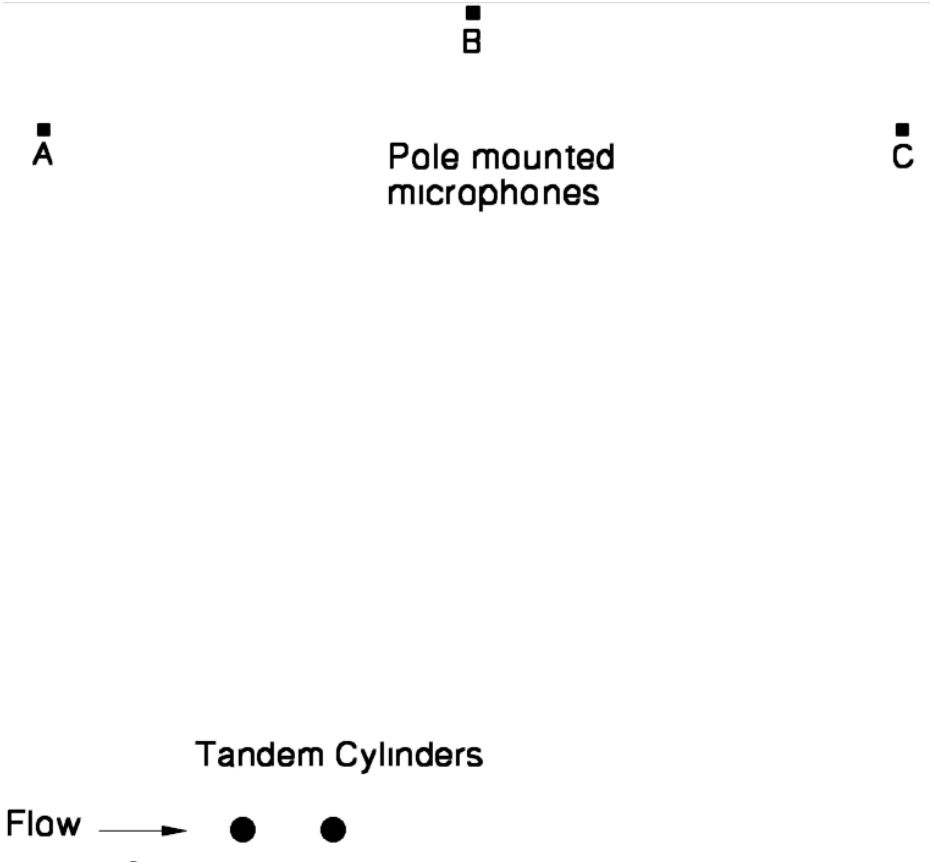

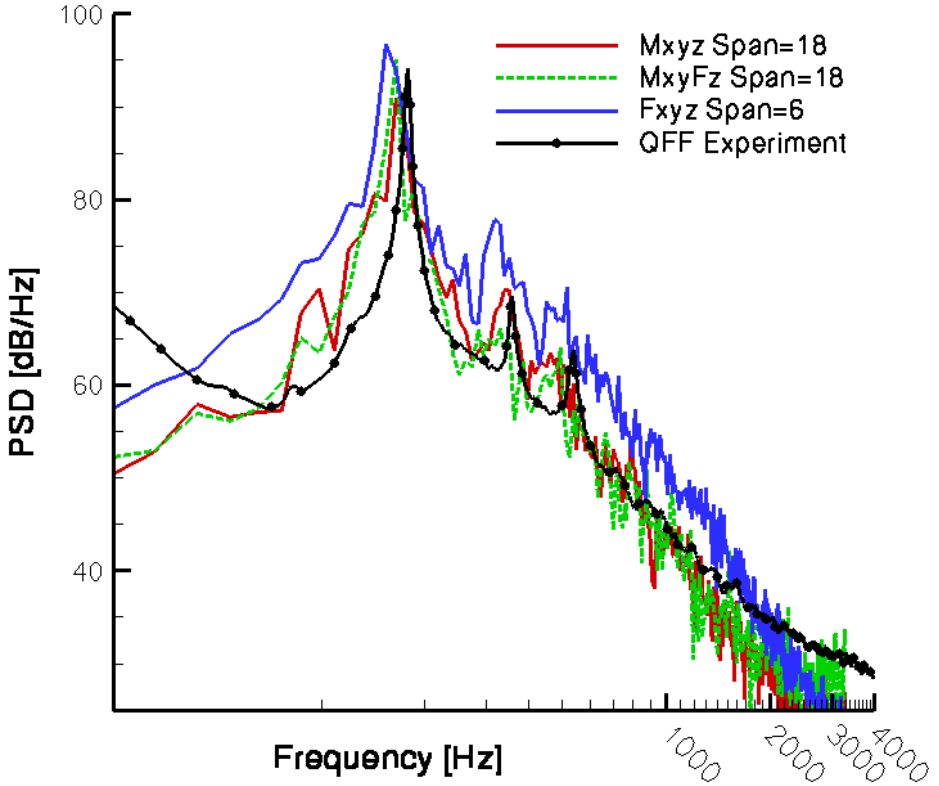

Spectra at A

Energy Stable WENO

- *Energy Stable* WENO (ESWENO)
  - A WENO-type scheme that is stable in the L_2 norm by construction for **continuous and discontinuous solutions**
- Developed New weights
  - Faster convergence to the underlying linear scheme
  - Improved shock-capturing capabilities
- Boundary Closures for 4th-order ESWENO
  - Design order accurate (3-4-3)

    Full stencil biasing up to boundaries (almost)

    L_2 Stability
- Maintains original properties
  - Design order of accuracy for smooth solutions/extrema
  - Conservative (Lax-Wendroff theorem)
  - Essentially nonoscillatory solutions

4th-order WENO Schemes

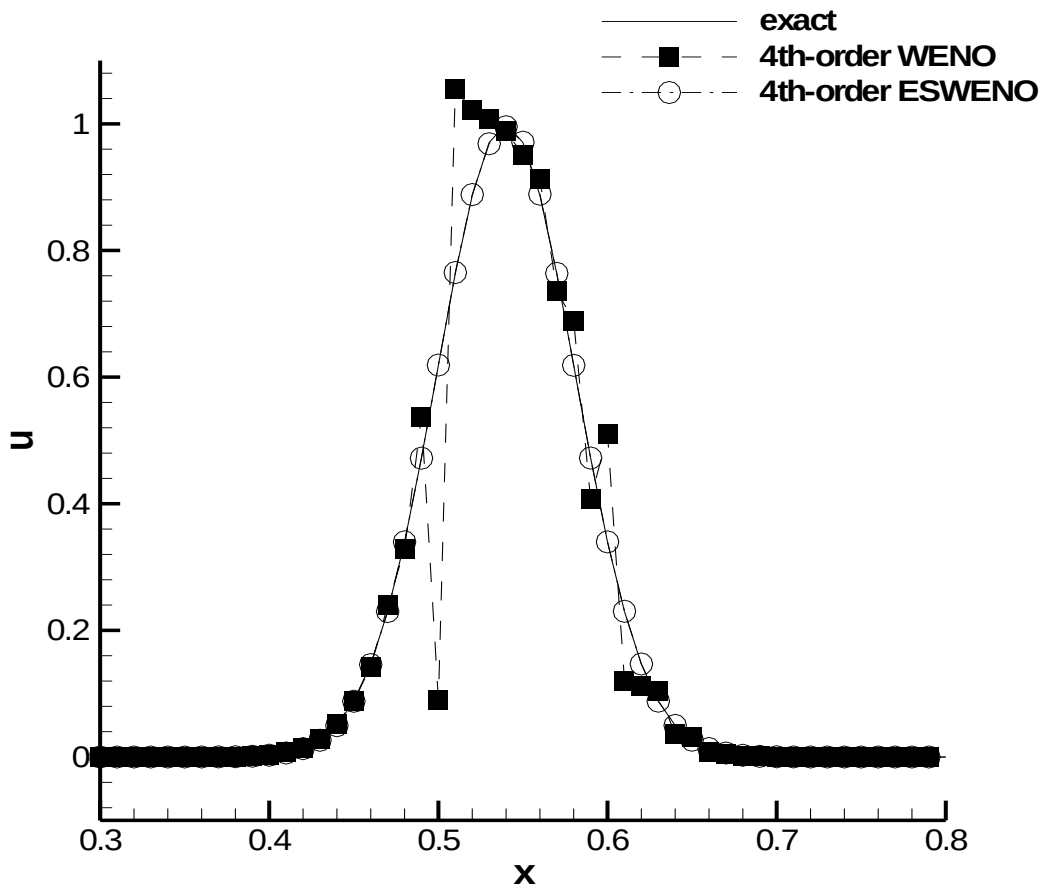

Solution obtained with the 4th-order WENO scheme for the linear wave equation with initial condition

$$u_0(x) = e^{-3.0(x-0.5)^2}$$

Numerical Results (cont.) *The Unsteady 1-D Euler Equations*

Shock/acoustic wave interaction problem , 5th and 6th-order WENO and ESWENO schemes (J=300 grid cells)

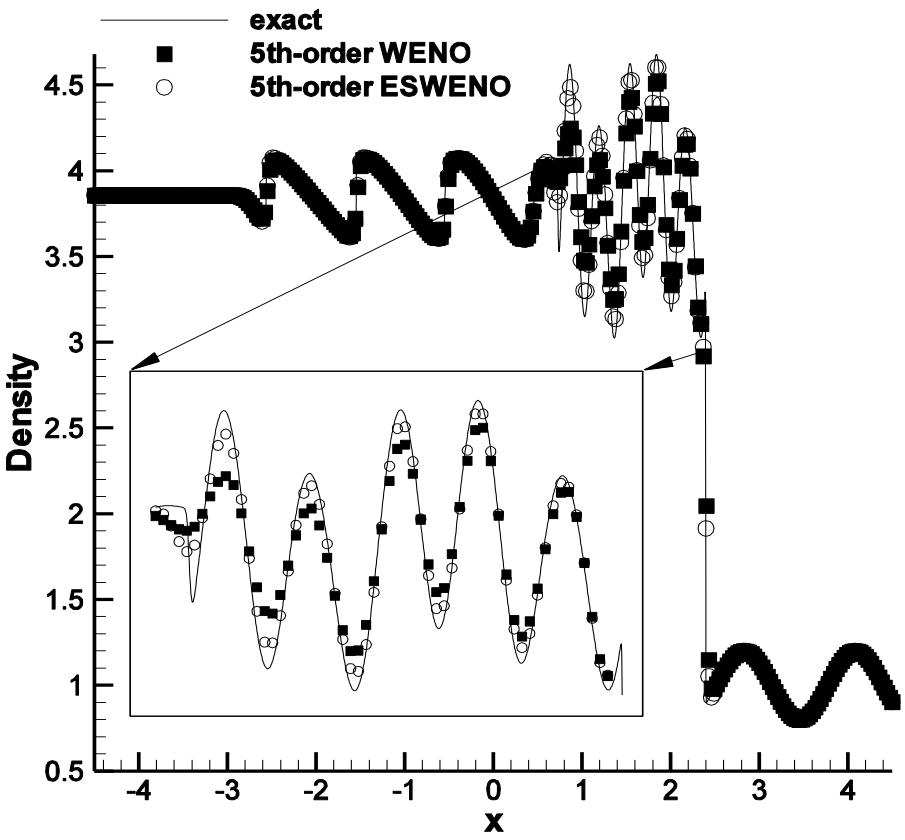

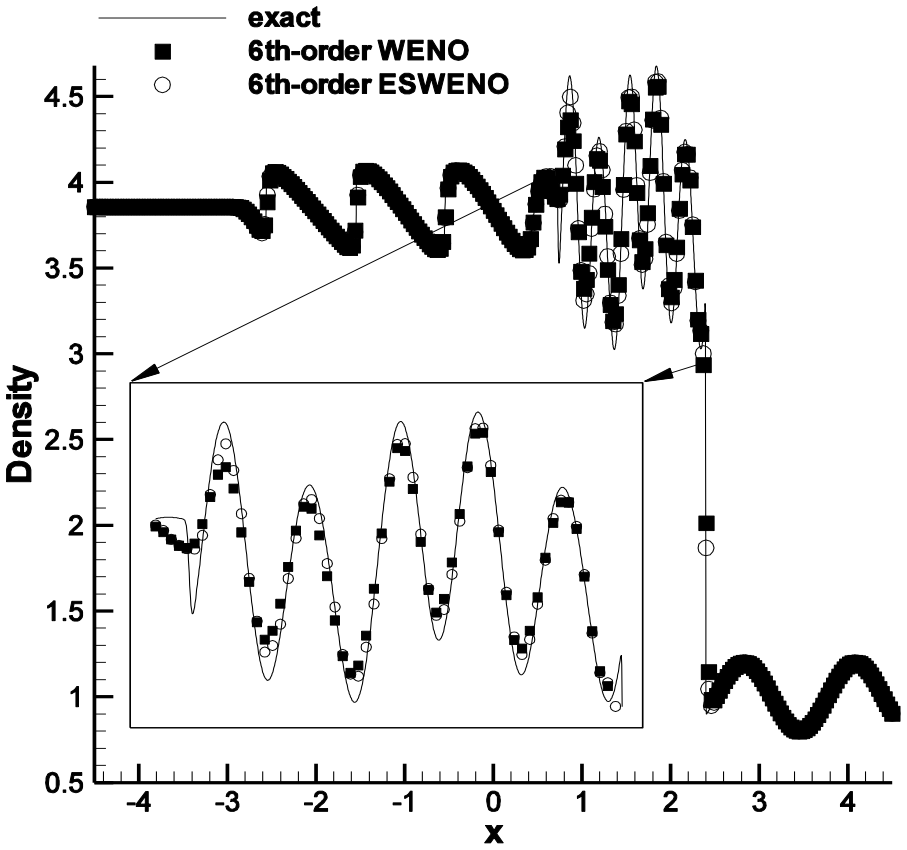

Numerical Results: Finite Domain

Euler isotropic vortex: ESWENO 4th(3-4-3)

	Linear Block Norm		$\text{ESWENO}_{3\text{-}4\text{-}3}$	
Number of Cells	**L_2 Error**	**L_2 Rate**	**L_2 Error**	**L_2 Rate**
50×50	2.49E-05	-	5.32E-05	-
100×100	1.64E-06	3.92	2.25E-06	4.57
200×200	1.04E-07	3.98	1.08E-07	4.37
400×400	6.57E-09	3.99	6.62E-09	4.04

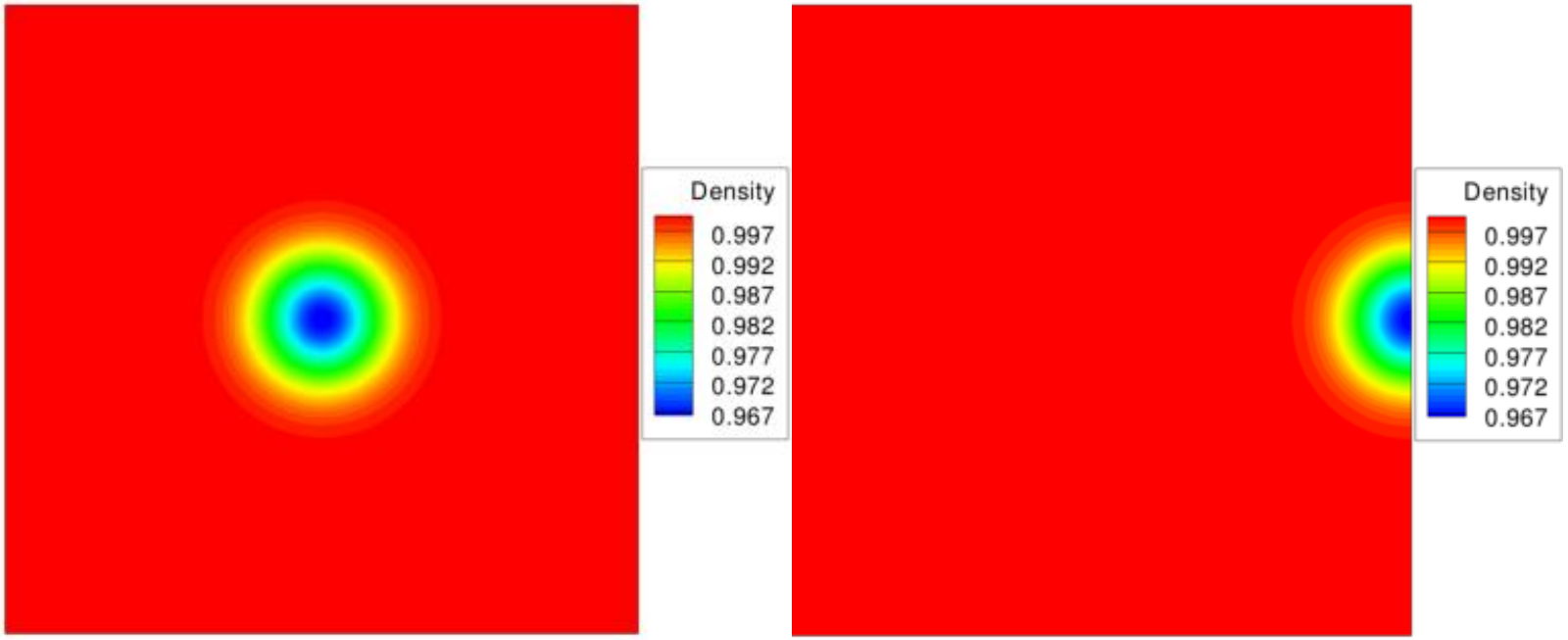

Numerical Results: Finite Domain 4th-order *ESWENO for Chemistry*

Compare Non-reacting and Reacting Mixing Layers

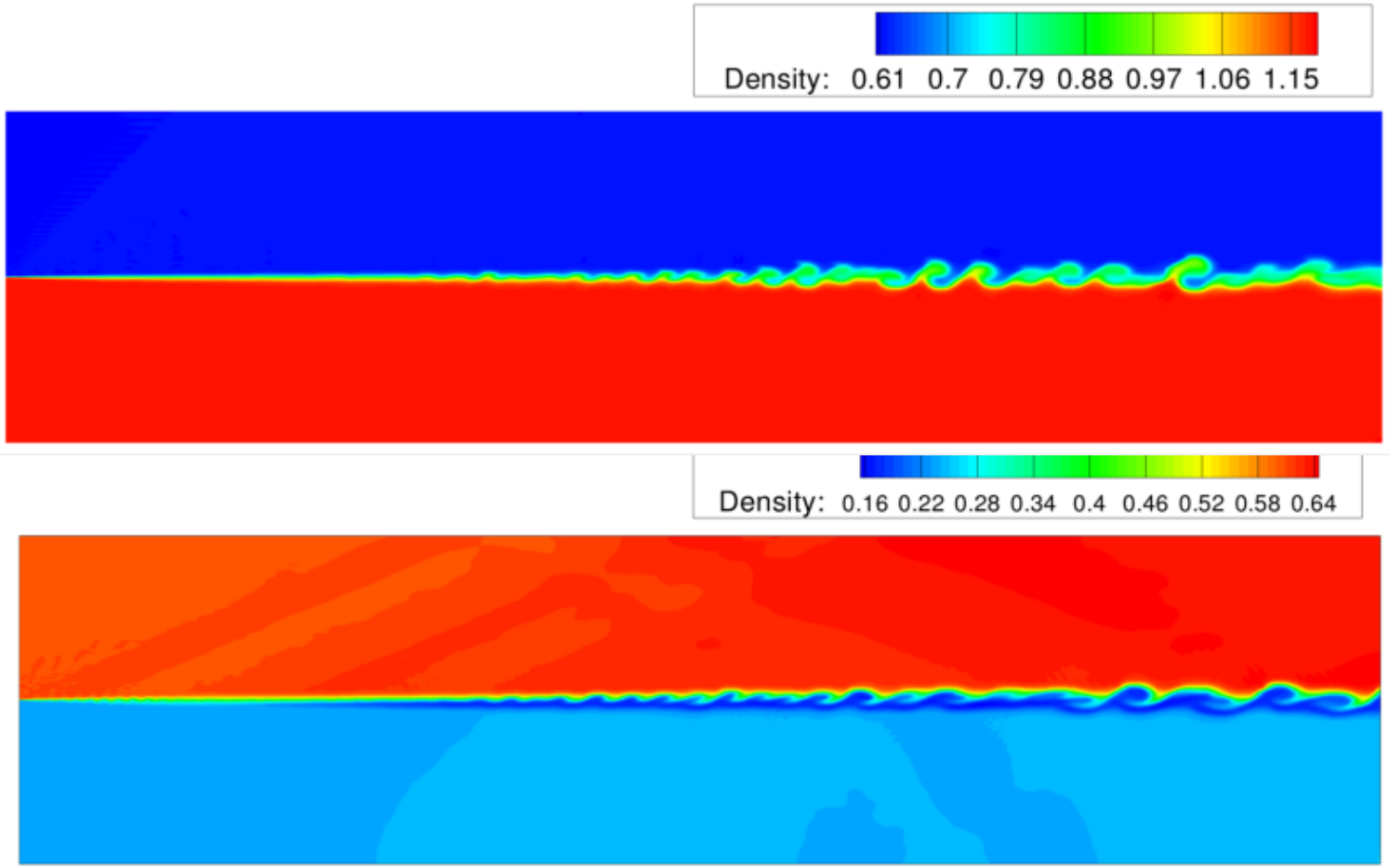

Summary for ESWENO

- The systematic methodology for constructing fourth-order ***finite domain Energy Stable WENO schemes*** is developed.
- We prove that for hyperbolic systems, the ***finite domain ESWENO*** scheme is ***stable in the energy norm*** for both continuous and ***discontinuous*** solutions.
- The eigenvalues of the finite domain ESWENO dissipation operator is located in the left-half plane.
- Based on the rigorous truncation error analysis, ***the new weight functions*** are developed, which ***drastically improve the accuracy*** of the ESWENO scheme and provide ***excellent shock-capturing capabilities***
- Numerical experiments show that the new finite domain ESWENO scheme with the new weights outperform the conventional WENO schemes in terms of accuracy.

BL Transition due to Streak Instabilities

Hyper-X Case Study (Choudhari et al. 2009)

- **Wind tunnel experiment** (Berry et al. 2001)

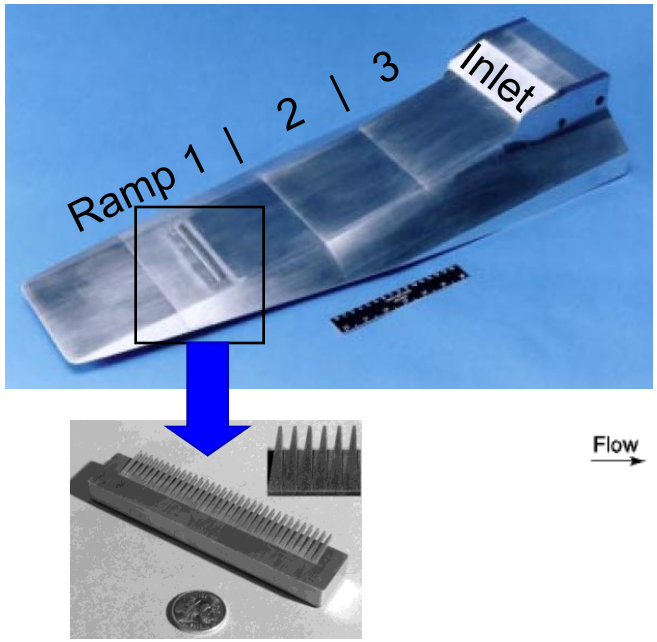

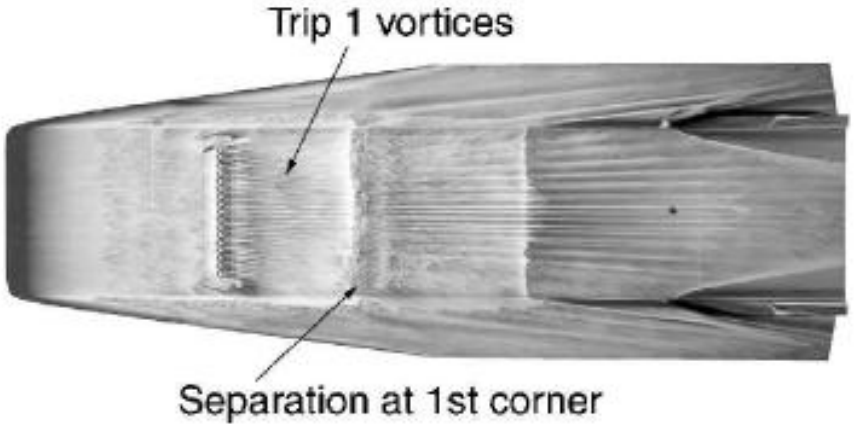

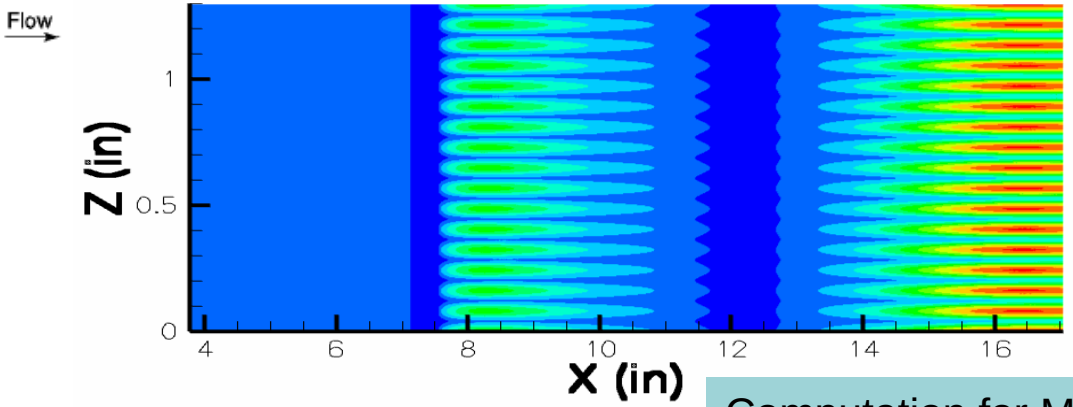

Computation for M = 6

- **k = 0.060" ⇒ k/δ ≈ 0.75 → Transition onset over ramp 1**
- **Heat transfer augmentation due to vortices/streaks**

Streak Mean Flow

- Flow settles into steady state; short separated region near trip array
- **Wake flow dominated by streamwise streaks** that persist for long distances
- Streak growth due to concave streamline curvature and transient growth?

Partial-differential Eigen-value problem

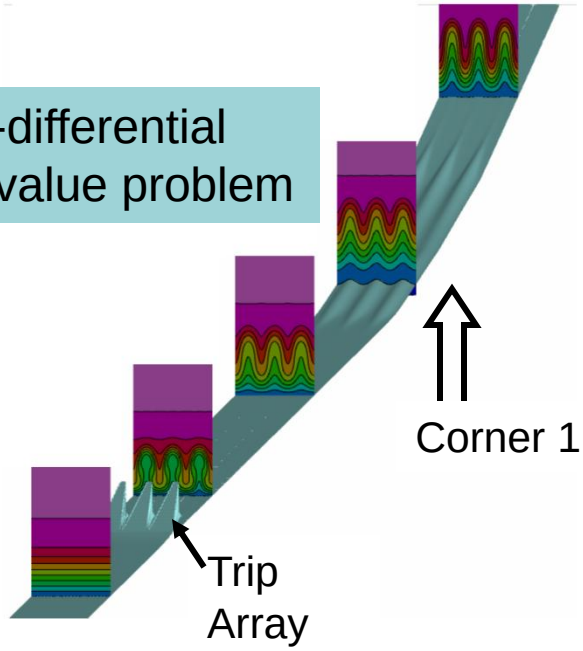

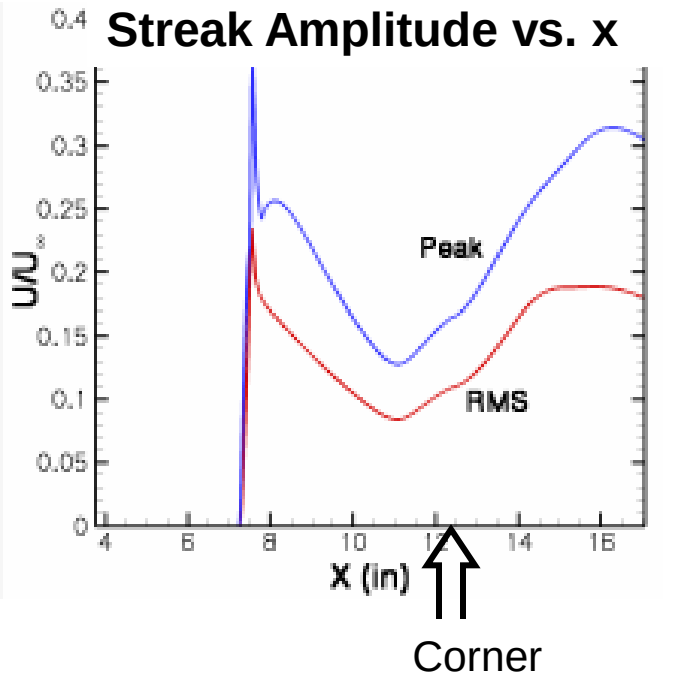

- Energized B.L. more resistant to separation

→ substantially weakened 3D separation bubble near 1st compression corner

Streak Instability Modes

(Similar to Gortler vortex secondary instabilities)

Sinuous

Varicose

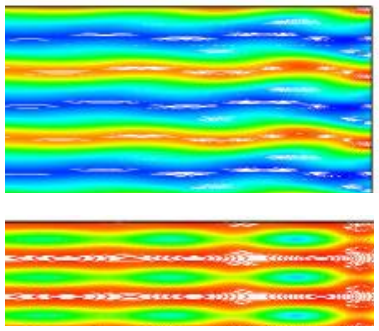

Mode 1, Z

Mode 2, Y

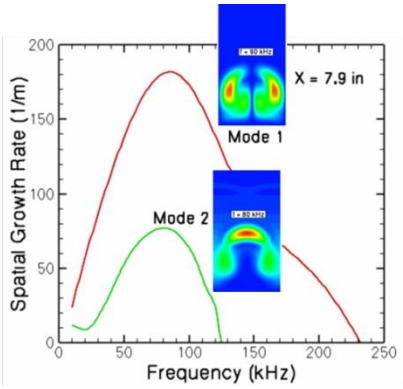

N factors

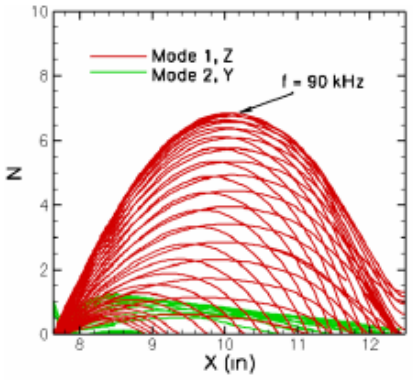

Ramp 1

Corner

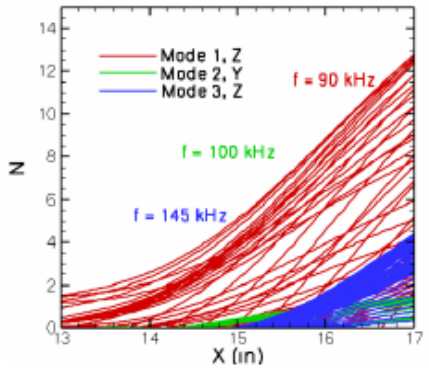

Ramp 2

-- Transition on Ramp 1 as N factor exceeds 7 for this conventional M = 6 tunnel
-- In general, transition could jump between Ramp 1 and 2 depending upon roughness height, shape, disturbance environment

Orbiter BLT Flight Experiment

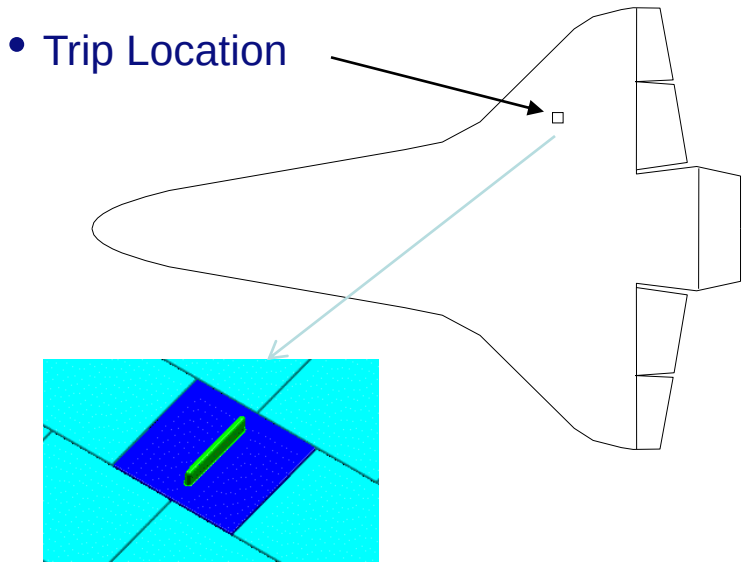

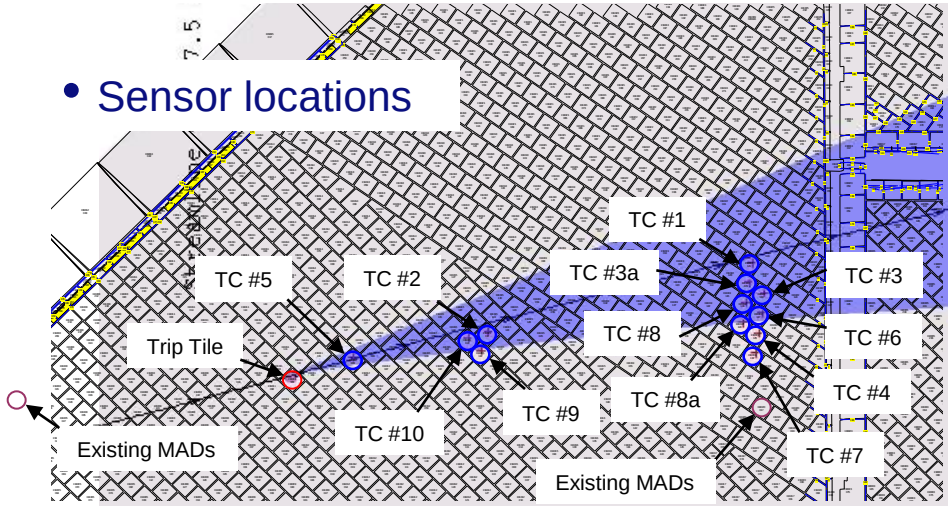

Slide courtesy of Scott Berry

- BLT experiment with fixed protuberances
  - Use 3 separate flights with incremental fixed heights (for flight envelope expansion)
    - ~0.25-in (Mach 15), ~0.5-in (Mach 17), and ~0.75-in (Mach 19)
- Global in-flight imaging of transition front (Horvath et al.)
- Streak instability a possible scenario?

Concluding Remarks

- A brief review of some of the CFD activities at NASA Langley has been given
  - *Grid Adaptation*
  - *Cell-centerd vs. Node-centered schemes*
  - *Multidimensional flux reconstruction*
  - *Design optimization using unsteady adjoints*
  - *High-order Methods*
  - *Unsteady simulations for noise source computation*
  - *BL transition research*